Acknowledgements—This study was supported in part by a grant from the Research Committee on Chorioretinal Degeneration and Optic Atrophy, Ministry of Health, Labor and Welfare (Dr. Sakamoto) and by a Grant-in-Aid for Scientific Research 19659452 from the Ministry of Education, Science and Culture, Japanese Government, Tokyo, Japan.

REFERENCES

Akassoglou K, Adams RA, Bauer J, Mercado P, Tseveleki V, Lassmann H, Probert L, Strickland S. Fibrin depletion decreases inflammation and delays the onset of demyelination in a tumor necrosis factor transgenic mouse model for multiple sclerosis. Proc Natl Acad Sci U S A 2004;101:6698–6703.

Alexandrov AV, Molina CA, Grotta JC, Garami Z, Ford SR, Alvarez-Sabin J, Montaner J, Saqqur M, Demchuk AM, Moye LA, Hill MD, Wojner AW. Ultrasound-enhanced systemic thrombolysis for acute ischemic stroke. N Engl J Med 2004;351:2170–2178.

Brown BS. How safe is diagnostic ultrasonography? Can Med Assoc J 1984;131:307–311.

Chater BV, Williams AR. Platelet aggregation induced *in vitro* by therapeutic ultrasound. Thromb Haemost 1977;38:640–651.

Cohen MG, Tuero E, Bluguermann J, Kevorkian R, Berrocal DH, Carlevaro O, Picabea E, Hudson MP, Siegel RJ, Douthat L, Greenbaum AB, Echt D, Weaver WD, Grinfeld LR. Transcutaneous ultrasound-facilitated coronary thrombolysis during acute myocardial infarction. Am J Cardiol 2003;92:454–457.

Coleman DJ, Lizzi FL, Driller J, Rosado AL, Burgess SE, Torpey JH, Smith ME, Silverman RH, Yablonski ME, Chang S, Rondeau MJ. Therapeutic ultrasound in the treatment of glaucoma. II. Clinical applications. Ophthalmology 1985;92:347–353.

Coleman DJ, Silverman RH, Iwamoto T, Lizzi FL, Rondeau MJ, Driller J, Rosado A, Abramson DH, Ellsworth RM. Histopathologic effects of ultrasonically induced hyperthermia in intraocular malignant melanoma. Ophthalmology 1988;95:970–981.

Daffertshofer M, Gass A, Ringleb P, Sitzer M, Sliwka U, Els T, Sedlaczek O, Koroshetz WJ, Hennerici MG. Transcranial low-frequency ultrasound-mediated thrombolysis in brain ischemia: Increased risk of hemorrhage with combined ultrasound and tissue plasminogen activator: Results of a phase II clinical trial. Stroke 2005;36:1441–1446.

Datta S, Coussios C-C, McAdory LE, Tan J, Porter T, de Courten-Myers G, Holland CK. Correlation of cavitation with ultrasound enhancement of thrombolysis. Ultrasound Med Biol 2006;32:1257–1267.

Drake MV. Neodymium:YAG laser iridotomy. Surv Ophthalmol 1987;32:171–177.

Feltgen N, Neubauer A, Jurklies B, Schmoor C, Schmidt D, Wanke J, Maier-Lenz H, Schumacher M. Multicenter study of the European Assessment Group for Lysis in the Eye (EAGLE) for the treatment of central retinal artery occlusion: Design issues and implications. EAGLE Study report no. 1: EAGLE Study report no. 1. Graefes Arch Clin Exp Ophthalmol 2006;244:950–956.

Francis CW, Onundarson PT, Carstensen EL, Blinc A, Meltzer RS, Schwarz K, Marder VJ. Enhancement of fibrinolysis *in vitro* by ultrasound. J Clin Invest 1992;90:2063–2068.

Francis CW, Blinc A, Lee S, Cox C. Ultrasound accelerates transport of recombinant tissue plasminogen activator into clots. Ultrasound Med Biol 1995;21:419–424.

Frenkel V, Oberoi J, Stone MJ, Park M, Deng C, Wood BJ, Neeman ZM III, Li KC. Pulsed high-intensity focused ultrasound enhances thrombolysis in an *in vitro* model. Radiology 2006;239:86–93.

Fukushima M, Nakashima Y, Sueishi K. Thrombin enhances release of tissue plasminogen activator from bovine corneal endothelial cells. Invest Ophthalmol Vis Sci 1989;30:1576–1583.

Garcia-Arumi J, Martinez-Castillo V, Boixadera A, Fonollosa A, Corcostegui B. Surgical embolus removal in retinal artery occlusion. Br J Ophthalmol 2006;90:1252–1255.

Hayreh SS, Zimmerman MB, Kimura A, Sanon A. Central retinal artery occlusion. Retinal survival time. Exp Eye Res 2004;78:723–736.

Hayreh SS. Intra-arterial thrombolysis for central retinal artery occlusion. Br J Ophthalmol 2008;92:585–587.

Holland CK, Vaidya SS, Datta S, Coussios C-C, Shaw GJ. Ultrasound-enhanced tissue plasminogen activator thrombolysis in an *in vitro* porcine clot model. Thromb Res 2008;121:663–673.

Hong AS, Chae JS, Dubin SB, Lee S, Fishbein MC, Siegel RJ. Ultrasonic clot disruption: An *in vitro* study. Am Heart J 1990;120:418–422.

Jaffe GJ, Schwartz D, Han DP, Gottlieb M, Hartz A, McCarty D, Mieler WF, Abrams GW. Risk factors for postvitrectomy fibrin formation. Am J Ophthalmol 1990;109:661–667.

Kattah JC, Wang DZ, Reddy C. Intravenous recombinant tissue-type plasminogen activator thrombolysis in treatment of central retinal artery occlusion. Arch Ophthalmol 2002;120:1234–1236.

Lauer CG, Burge R, Tang DB, Bass BG, Gomez ER, Alving BM. Effect of ultrasound on tissue-type plasminogen activator-induced thrombolysis. Circulation 1992;86:1257–1264.

McDonald HR, Schatz H, Johnson RN. Postoperative intraocular fibrin formation is a potentially disastrous complication of vitrectomy surgery. Retina 1990;10:317–318.

Noble J, Weizblit N, Baerlocher MO, Eng KT. Intra-arterial thrombolysis for central retinal artery occlusion: A systematic review. Br J Ophthalmol 2008;92:588–593.

Opremcak E, Rehmar AJ, Ridenour CD, Borkowski LM, Kelley JK. Restoration of retinal blood flow *via* translumenal Nd:YAG embolysis/embolectomy (TYL/E) for central and branch retinal artery occlusion. Retina 2008;28:226–235.

Pfaffenberger S, Devcic-Kuhar B, Kastl SP, Huber K, Maurer G, Wojta J, Gottsauner-Wolf M. Ultrasound thrombolysis. Thromb Haemost 2005;94:26–36.

Richard G, Lerche RC, Knospe V, Zeumer H. Treatment of retinal arterial occlusion with local fibrinolysis using recombinant tissue plasminogen activator. Ophthalmology 1999;106:768–773.

Saito K, Miyake K, McNeil PL, Kato K, Yago K, Sugai N. Plasma membrane disruption underlies injury of the corneal endothelium by ultrasound. Exp Eye Res 1999;68:431–437.

Sakamoto T, Oshima Y, Nakagawa K, Ishibashi T, Inomata H, Sueishi K. Target gene transfer of tissue plasminogen activator to cornea by electric pulse inhibits intracameral fibrin formation and corneal cloudiness. Hum Gene Ther 1999;10:2551–2557.

Sonoda S, Tachibana K, Uchino E, Okubo A, Yamamoto M, Sakoda K, Hisatomi T, Sonoda KH, Negishi Y, Izumi Y, Takao S, Sakamoto T. Gene transfer to corneal epithelium and keratocytes mediated by ultrasound with microbubbles. Invest Ophthalmol Vis Sci 2006;47:558–564.

Tachibana K. Enhancement of fibrinolysis with ultrasound energy. J Vasc Intervent Radiol 1992;3:299–303.

Tachibana K, Tachibana S. Albumin microbubble echo-contrast material as an enhancer for ultrasound accelerated thrombolysis. Circulation 1995;92:1148–1150.

Tachibana K, Tachibana S. Prototype therapeutic ultrasound emitting catheter for accelerating thrombolysis. J Ultrasound Med 1997;16:529–535.

Tomey KF, Traverso CE, Shammas IV. Neodymium-YAG laser iridotomy in the treatment and prevention of angle closure glaucoma. A review of 373 eyes. Arch Ophthalmol 1987;105:476–481.

Toth CA, Morse LS, Hjelmeland LM, Landers MB III. Fibrin directs early retinal damage after experimental subretinal hemorrhage. Arch Ophthalmol 1991;109:723–729.

Trubestein G, Engel C, Etzel F, Sobbe A, Cremer H, Stumpff U. Thrombolysis by ultrasound. Clin Sci Mol Med Suppl 1976;3:697s–698s.

Vine AK, Samama MM. The role of abnormalities in the anticoagulant and fibrinolytic systems in retinal vascular occlusions. Surv Ophthalmol 1993;37:283–292.

Weber J, Remonda L, Mattle HP, Koerner U, Baumgartner RW, Sturzenegger M, Ozdoba C, Koerner F, Schroth G. Selective intra-arterial fibrinolysis of acute central retinal artery occlusion. Stroke 1998;29:2076–2079.

White WM, Makin IR, Slayton MH, Barthe PG, Gliklich R. Selective transcutaneous delivery of energy to porcine soft tissues using Intense Ultrasound (IUS). Lasers Surg Med 2008;40:67–75.

Yamamoto T, Kamei M, Kunavisarut P, Suzuki M, Tano Y. Increased retinal toxicity of intravitreal tissue plasminogen activator in a central

retinal vein occlusion model. Graefes Arch Clin Exp Ophthalmol 2008;246:509–514.

Yamashita T, Sonoda S, Suzuki R, Arimura N, Tachibana K, Maruyama K, Sakamoto T. A novel bubble liposome and ultrasound-mediated gene transfer to ocular surface: RC-1 cells in vitro and conjunctiva *in vivo*. Exp Eye Res 2007;85:741–748.

Yoeruek E, Spitzer MS, Tatar O, Biedermann T, Grisanti S, Luke M, Bartz-Schmidt KU, Szurman P. Toxic effects of recombinant tissue plasminogen activator on cultured human corneal endothelial cells. Invest Ophthalmol Vis. Sci 2008;49:1392–1397.

Zderic V, Clark JI, Vaezy S. Drug delivery into the eye with the use of ultrasound. J Ultrasound Med 2004;23:1349–1359.

THE JOURNAL OF BIOLOGICAL CHEMISTRY VOL. 284, NO. 14, pp. 9147–9152, April 3, 2009

Characterization of N-terminal Structure of TLR2-activating Lipoprotein in *Staphylococcus aureus*[*]

Received for publication, January 21, 2009 Published, JBC Papers in Press, February 13, 2009, DOI 10.1074/jbc.M900429200

Kazuki Tawaratsumida[‡], Maiko Furuyashiki[§], Mami Katsumoto[¶], Yukari Fujimoto[¶], Koichi Fukase[¶], Yasuo Suda[‡], and Masahito Hashimoto[‡1]

From the [‡]Department of Nanostructure and Advanced Materials and [§]Venture Business Laboratory, Kagoshima University, Korimoto 1-21-40, Kagoshima 890-0065 and the [¶]Department of Chemistry, Graduate School of Science, Osaka University, Toyonaka, Osaka 560-0043, Japan

Staphylococcus aureus **is known to activate mammalian immune cells through Toll-like receptor 2 (TLR2). We recently demonstrated that a lipoprotein fraction obtained from *S. aureus* by Triton X-114 phase partitioning is a potent activator of TLR2. In this study, we separated TLR2-activating lipoproteins expressed in *S. aureus* and characterized an N-terminal structure. The lipoprotein fraction of *S. aureus* was prepared by glass bead disruption followed by Triton X-114 phase partitioning. The TLR2-activating molecules were mainly detected in the mass range of 30–35 kDa. Seven lipoproteins were identified by the mass spectra of their tryptic digests. Among them, three lipoproteins were separated by preparative SDS-PAGE and proved to activate TLR2. After digestion with trypsin in the presence of sodium deoxycholate, the N terminus of the lipopeptide was isolated from lipoprotein SAOUHSC_02699 by normal phase high pressure liquid chromatography and characterized as an *S*-(diacyloxypropyl)cystein-containing peptide using tandem mass spectra. The synthetic lipopeptide counterpart also stimulated the cells via TLR2. These results showed that the diacylated lipoprotein from *S. aureus* acts as a TLR2 ligand in mammalian cells.**

Bacterial infection is one of the major causes of death. *Staphylococcus aureus*, the most common Gram-positive pathogen, is a major source of mortality in medical facilities (1). The pathogen causes various infectious diseases, including sepsis, endocarditis, and pneumonia. During the infection, *S. aureus* activates cells and evokes serious inflammation in the host. TLR2 [2] has been shown to play a crucial role in the host response to *S. aureus* (2). However, a detailed understanding of the molecular components that interact with TLR2 in *S. aureus* cells has not yet been obtained. One of the reported TLR2 ligands was peptidoglycan (PGN) (3), a cell wall component of most bacteria. However, Travassos *et al.* (4) recently showed that PGN from several bacteria that were highly purified by removal of lipoproteins or lipoteichoic acid (LTA) were not detected by TLR2. Moreover, the minimal active components of the PGN, muramyl dipeptide and desmuramyl dipeptide (γ-D-glutamyl diaminopimelic acid), were determined to be ligands of the intracellular innate immune receptor Nod2/Nod1 (5, 6), suggesting that PGN is not a ligand of TLR2. Another candidate of TLR2-activating ligands is LTA, a cell surface glycoconjugate of Gram-positive bacteria (3). Morath *et al.* (7) reported that LTA from *S. aureus* is a potent stimulator of cytokine release, whereas our group demonstrated that LTA from enterococci, also a major Gram-positive pathogen, has no cytokine-producing activity (8, 9). Furthermore, Han *et al.* (10) showed that LTA from pneumococci is 100-fold less potent than staphylococcal LTA. These observations suggested that LTA is not a common ligand of TLR2 in Gram-positive pathogens.

We also found that the enterococcal LTA fraction contains some contaminants other than LTA and that these components activate immune cells through TLR2 (8, 11). However, their structures were not identified at that time. TLR2 is known to be a predominant receptor for lipoproteins derived from various bacteria. We have previously shown that the lipoprotein-containing fraction from *S. aureus* stimulates activation of immune cells through TLR2 (12). Recently, Stoll *et al.* (13) constructed a lipoprotein diacylglycerol transferase deletion (Δ*lgt*) mutant of *S. aureus*, which is unable to carry out lipid modification of prelipoproteins. It was demonstrated that the mutant completely lacks palmitate-labeled lipoproteins and that its cells and crude lysate induce much less proinflammatory cytokines than the wild type. Bubeck *et al.* (14) also reported that an *S. aureus* variant that lacks lipoproteins is able to escape immune recognition and cause lethal infections. Furthermore, we showed that the activities of an LTA fraction derived from a Δ*lgt* mutant are largely decreased when compared with those from the same fraction of the wild type (15). These results suggest that the lipoproteins in *S. aureus* appear to be the TLR2 ligand for the immune system. In the present study, we separated lipoproteins from *S. aureus* and elucidated the TLR2-activating structure.

EXPERIMENTAL PROCEDURES

Bacterial Strain and Bacterial Components—*S. aureus* SA113, a restriction-deficient mutant of NCTC8325 (16), was cultured in brain heart infusion broth (Eiken, Tokyo, Japan) at 37 °C for 6 h with constant shaking in a culture bag (CB20-1, Fujimori Kogyo Co., Ltd., Tokyo, Japan) before being harvested by cen-

* This work was supported by a research grant from The Uehara Memorial Foundation.

[1] To whom correspondence should be addressed. Tel./Fax: 81-99-285-7742. E-mail: hassy@eng.kagoshima-u.ac.jp.

[2] The abbreviations used are: TLR, Toll-like receptor; mTLR2, murine TLR2; LTA, lipoteichoic acid; MALDI-TOF-MS, matrix-assisted laser desorption ionization-time of flight mass spectrometry; MS/MS, tandem mass spectrometry; PBMC, peripheral blood mononuclear cell; PGN, peptidoglycan; HPLC, high pressure liquid chromatography; TNF, tumor necrosis factor.

trifugation (5,000 × *g* for 15 min at 4 °C). The membrane fraction was prepared by bead disruption of the cells as described (13). The lipoprotein fraction was obtained by Triton X-114 phase partitioning of the membrane fraction as described (17) and was designated as Sa-M-TX.

FSL-1, a synthetic diacylated lipopeptide, was purchased from EMC microcollections (Tübingen, Germany). *Escherichia coli* O55:B5 lipopolysaccharide (Sigma-Aldrich) was further purified by sodium deoxycholate reextraction as described (18). SAOUHSC_02699 di-*O*-palmitoyl (Pam_2) lipopeptide 10-mer (Pam_2CGNNSSKDKDG) and Pam_2CSK_4 were synthesized in our laboratory. The synthetic details will be described elsewhere.

Separations of Proteins—Analytical SDS-PAGE was performed by the Tris-glycine method (19) using a mini PAGE chamber AE-6530 and an AE-8450 power supply (Atto Corp., Tokyo, Japan) with a 12.5% gel. Proteinous materials were visualized by silver or Coomassie Brilliant Blue staining, and visualization of acidic materials, such as LTA, was performed by Alcian blue staining.

Proteins eluting between 25 and 40 kDa in the analytical SDS-PAGE were separated using a preparative electrophoresis apparatus, AE-6750 (Atto Corp.), according to the manufacturer's instructions. The eluates were analyzed by SDS-PAGE and subjected to acetone precipitation to remove any contaminating SDS. The precipitates were dissolved in 20 mM octylglucoside. The concentration of lipoprotein was estimated by SDS-PAGE with silver staining and adjusted to 10 μg/ml.

Monocyte Western Blotting—Monocyte Western blotting was carried out by the method described previously (20). Briefly, stimuli were separated by SDS-PAGE, and the resolved stimuli in the gel were transblotted to a nitrocellulose membrane by the method of Towbin *et al.* (21) using an AE-6677 semidry blotting apparatus (Atto Corp.). The membrane of each lane was cut into 4-mm strips, and each strip was separately dissolved in dimethyl sulfoxide. The solution was poured into phosphate-buffered saline to precipitate stimuli-coated particles, which consist of stimuli and nitrocellulose. After washing three times with phosphate-buffered saline, the particle suspension in assay medium was applied to a luciferase assay using the Ba/mTLR2 cells described below.

Mass Spectrometry—Mass spectra were obtained by matrix-assisted laser desorption ionization-time of flight mass spectrometry (MALDI-TOF-MS) with an Axima QIT TOF mass spectrometer (Shimadzu, Kyoto, Japan) equipped with a nitrogen 337 nm laser. 2,5-Dihydroxybenzoic acid was used as the matrix at a concentration of 10 mg/ml in aqueous 50% acetonitrile containing 0.1% trifluoroacetic acid. Peptides were analyzed in positive and reflectron mode. Tandem mass (MS/MS) spectra were obtained using argon as a collision gas.

Identification of Lipoproteins and Lipopeptides—The proteins that were separated by analytical SDS-PAGE were digested with trypsin as described previously (22). The peptides were analyzed by MALDI-TOF-MS and identified by a data base (the National Center for Biotechnology Information nonredundant protein data base) search using the MASCOT software from Matrix Science (23). The proteins were designated

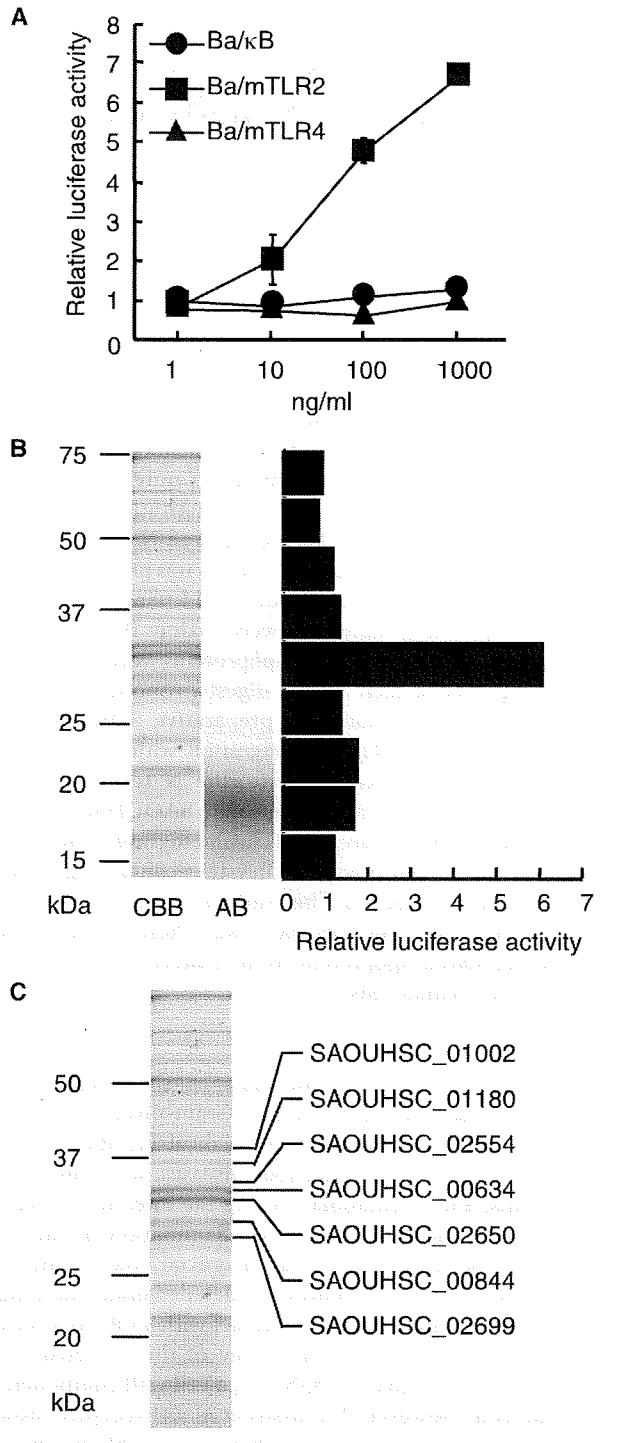

FIGURE 1. **Identification of lipoproteins in *S. aureus*.** *A*, the NF-κB activation induced by Sa-M-TX in Ba/κB, Ba/mTLR2, or Ba/mTLR4/mMD-2 cells for 4 h was measured with a luciferase assay. The results are shown as relative luciferase activity, which was determined as the ratio of stimulated to nonstimulated activity. The data represent the mean ± S.E. obtained from three independent experiments. *B*, SDS-PAGE profiles of Sa-M-TX and separation of TLR2-activating components in Sa-M-TX. The gels were separated with 12.5% gel and visualized by Coomassie Brilliant Blue (*CBB*) or Alcian blue (*AB*). NF-κB activation was detected by monocyte Western blotting using a luciferase assay in Ba/mTLR2 cells. The results are shown as relative luciferase activity, which was determined as the ratio of stimulated to nonstimulated activity. *C*, identification of lipoproteins in Sa-M-TX. Each protein were separated with 12.5% gel and identified by in-gel tryptic digestion followed by mass analysis.

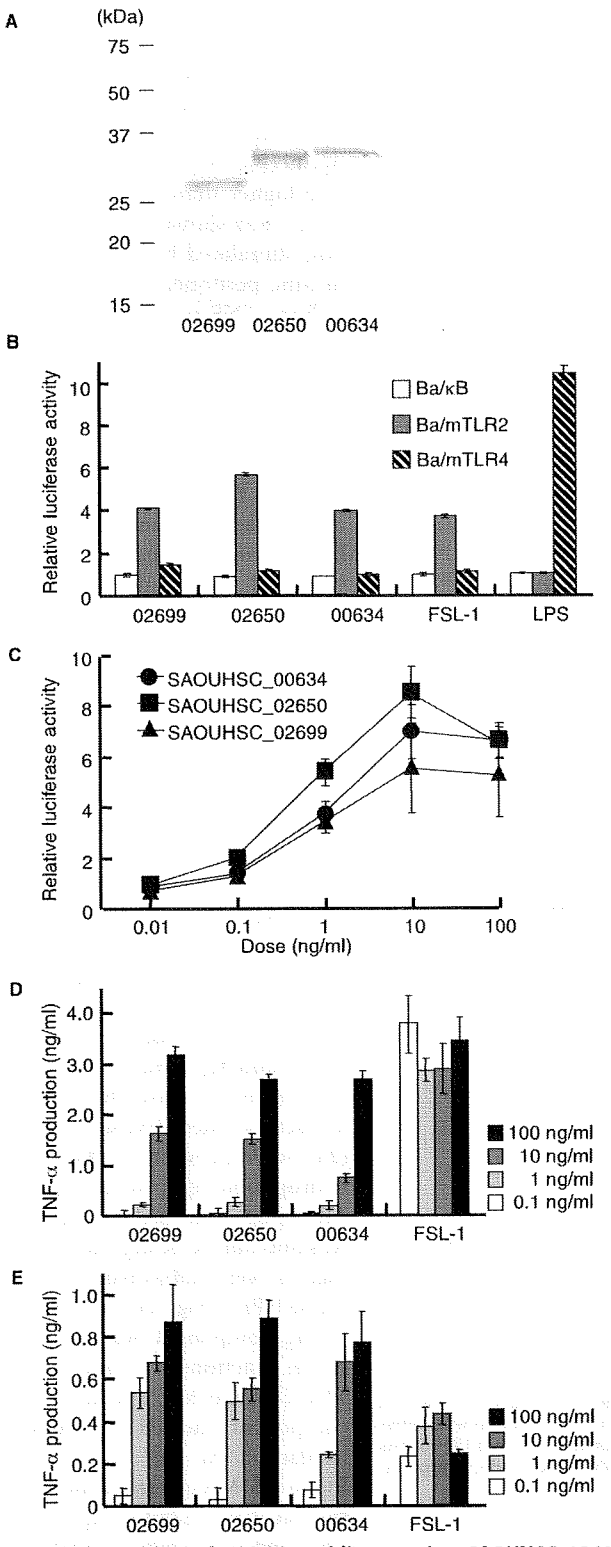

FIGURE 2. **Immunological activities of lipoproteins, SAOUHSC_02699, -02650, and -00634 separated by preparative SDS-PAGE using 12.5% gel.** *A*, SDS-PAGE profile of lipoproteins. They were separated in 12.5% gel and visualized by silver staining. *B*, the NF-κB activation induced by 1 ng/ml of the lipoprotein, 0.1 ng/ml FSL-1, and 10 ng/ml lipopolysaccharide (*LPS*) in Ba/κB, Ba/mTLR2, or Ba/mTLR4/mMD-2 cells. *C*, dose-dependent NF-κB activation induced by lipoproteins in Ba/mTLR2 cells. The cells were incubated with stimuli for 4 h. NF-κB activation was measured with a luciferase assay. The results are shown as relative luciferase activity, which was determined as the ratio of stimulated to nonstimulated activity. The data represent the mean ± S.E. obtained from three independent experiments. *D*, TNF-α production induced by the lipoprotein in human PBMC. *E*, TNF-α production induced by the lipoprotein in murine peritoneal exudate cells. The levels of TNF-α in the culture supernatants of the cells incubated with the indicated concentration of the stimuli for 4 h were measured by enzyme-linked immunosorbent assay. The data represent the mean ± S.E. obtained from three independent experiments.

by the locus tags for the genome of *S. aureus* NCTC8325, which is the parent strain of SA113 (16).

To isolate the N-terminal lipopeptide, the lipoprotein fraction was subjected to phase transfer surfactant-aided trypsin digestion (24). The tryptic digest was subjected to HPLC using a normal phase Daisopak SP-120-5-SIL-P column (250 × 4.6 mm, DAISO, Co., Ltd., Osaka, Japan). The digests were eluted using a gradient program (solvent A, chloroform, methanol, water = 65/20/3, v/v/v; solvent B, chloroform, methanol, water = 65/40/3, v/v/v) at a flow rate of 1.0 ml/min and were fractionated into 1-ml portions. The N-terminal lipopeptide was detected using a luciferase assay. The purified lipopeptide was characterized by MALDI-TOF-MS.

Luciferase Assay—Ba/F3 cells that stably expressed p55IgκLuc, an NF-κB/DNA binding activity-dependent luciferase reporter construct (Ba/κB), murine TLR2 and the p55IgκLuc reporter construct (Ba/mTLR2), and murine TLR4/MD-2 and the p55IgκLuc reporter construct (Ba/mTLR4/mMD-2) were kindly provided by Prof. K. Miyake (Institute of Medical Science, University of Tokyo, Japan). The NF-κB-dependent luciferase activity in these cells was determined as described previously (12).

Cytokine Assay—Eight-week-old male BALB/c mice were obtained from Kyudo (Kumamoto, Japan). The animals received humane care in accordance with our institutional guidelines and the legal requirements of Japan. Stimulation of thioglycolate-elicited peripheral exudate cells and Histopaque-separated human peritoneal blood mononuclear cells (PBMC) from a healthy donor (M. F.) and a cytokine assay for secreted murine or human TNF-α were performed as described (15).

RESULTS

Identification of Lipoproteins in S. aureus—The lipoprotein fraction was obtained from *S. aureus* cells using glass bead disruption followed by Triton X-114 phase partitioning. Four mg of the lipoprotein fraction (Sa-M-TX) were obtained from 10 liters of bacterial cell culture. Sa-M-TX activated murine TLR2 expressing cells (Ba/mTLR2) at 10 ng/ml but not murine TLR4 and MD-2 expressing Ba/mTLR4/mMD-2 cells or the negative control Ba/κB cells (Fig. 1*A*). The SDS-PAGE profile of Sa-M-TX showed that it contained Coomassie Brilliant Blue (*CBB*)-positive proteins and Alcian blue (*AB*)-positive components (Fig. 1*B*). The active molecules in Sa-M-TX were analyzed by monocyte Western blotting. TLR2-mediated NF-κB activation was strongly detected in a molecular mass range of 30–35 kDa (Fig. 1*B*). Thus, we subjected the Sa-M-TX proteins with molecular masses of around 30–35 kDa to in-gel tryptic digestion. At least seven lipoproteins, SAOUHSC_00634, -00844, -01002, -01180, -02554, -02650, and -02699, were identified by a combination of peptide mass fingerprinting and MS/MS spectra (Fig. 1*C*).

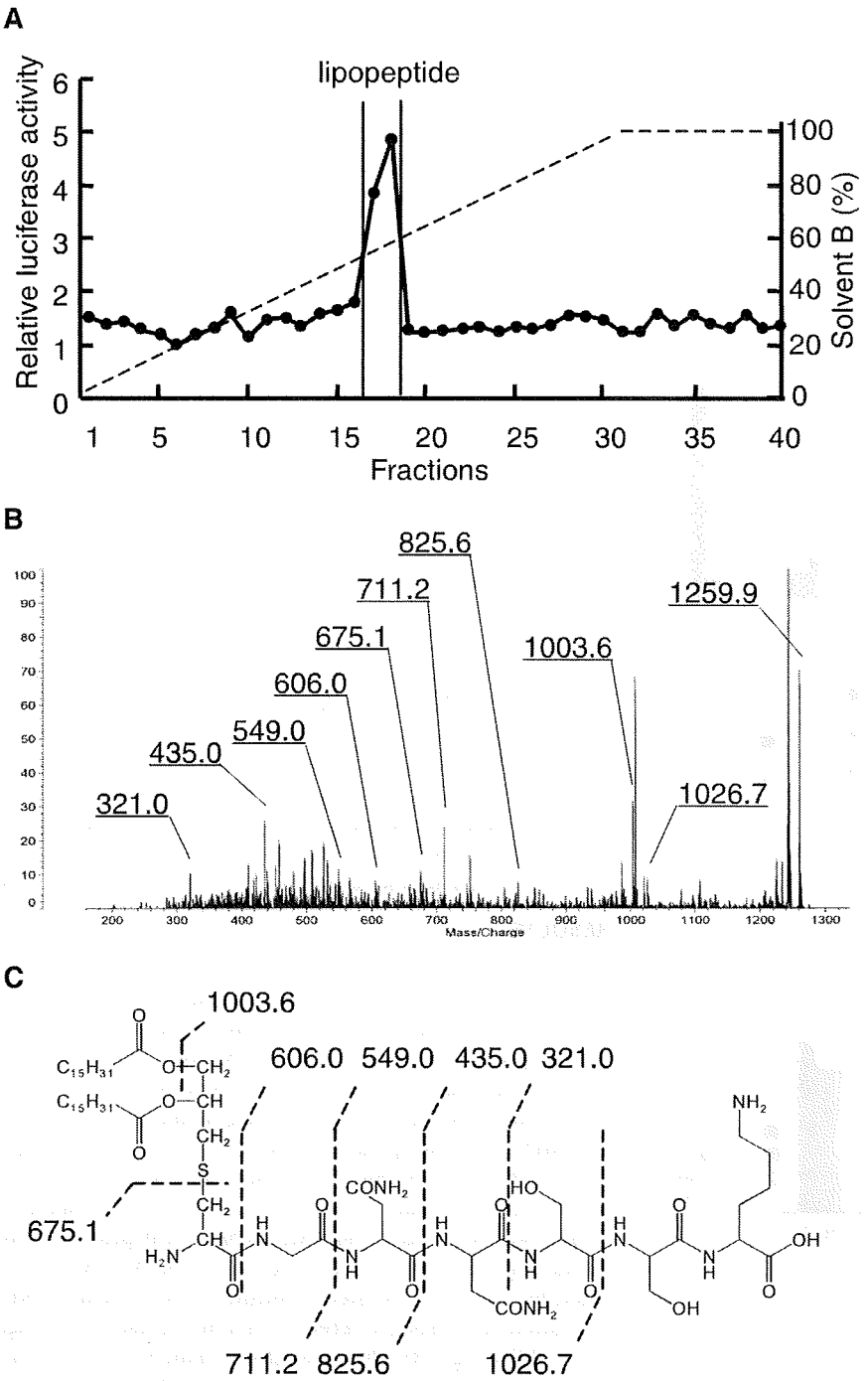

FIGURE 3. **Characterization of the N-terminal lipopeptide of SAOUHSC_02699.** *A*, the elution profile of a tryptic digest of SAOUHSC_02699 using normal phase HPLC. The NF-κB activation of the fraction was determined using Ba/mTLR2 cells. *B*, the MS/MS spectrum of the lipopeptide. The precursor ion at *m/z* 1259.9 was decomposed using collision-induced dissociation (CID) mode. *C*, the structure of the lipopeptide. Interpretations of the fragment ions in the MS/MS spectra are indicated in the structure.

Lipoprotein Immunological Activities—The lipoproteins were separated by preparative SDS-PAGE using a 12.5% gel. Among seven identified lipoproteins, we could separate three lipoproteins, SAOUHSC_02699, -02650, and -00634 (Fig. 2*A*). About 1 μg of each lipoprotein were obtained from 250 μg of Sa-M-TX. The TLR2-dependent activities of the lipoproteins were detected by NF-κB activation in TLR-expressing cells. All lipoproteins induced NF-κB activation in Ba/mTLR2 cells but not in Ba/mTLR4/mMD-2 or Ba/κB cells (Fig. 2*B*). The activities of the lipoproteins were observed at 0.1 ng/ml (Fig. 2*C*) and were about 100-fold higher than that of Sa-M-TX, which was shown in Fig. 1*A*. They also stimulated human PBMC and murine peritoneal exudate cells to induce TNF-α dose dependently (Fig. 2, *D* and *E*). The other four lipoproteins could not be analyzed because of the low content in Sa-M-TX.

The N-terminal Structure of S. aureus Lipoprotein—Because the minimal active structure of bacterial lipoproteins is reported to be N-terminal acylated *S*-(2,3-dihydroxypropyl)cysteine-containing lipopeptide (25), the N-terminal structure of *S. aureus* lipoprotein was investigated. We attempted to separate N-terminal lipopeptides from three separated lipoproteins by conventional tryptic digestion followed by reverse or normal phase HPLC separation. Although active components were eluted, no lipopeptides were detected by mass spectrometry. This may have been caused by insufficient digestion of the N-terminal moiety of the lipopeptides, probably because of poor solubility or micelle formation. Therefore, we used phase transfer surfactant-aided trypsin digestion (24) to improve the efficiency of hydrophobic lipoprotein digestion. The lipoprotein SAOUHSC_02699 was thus able to be digested, and the digests were subjected to normal phase HPLC (Fig. 3*A*). A TLR2-activating component was found between fractions 17 and 18. The MALDI-TOF-MS spectra of the component showed a pseudomolecular ion $[M+H]^+$ at *m/z* 1259.9. In the MS/MS spectra of the precursor ion at *m/z* 1259.9 (Fig. 3, *B* and *C*), C-terminal y ions were observed at *m/z* 606.0, 549.0, 435.0, and 321.0, which agreed with the N-terminal sequence of SAOUHSC_02699, GNNSSK. The ions at *m/z* 1026.7, 825.6, and 711.2 correspond to b ions of an *S*-(dipalmitoyloxypropyl)-cysteine-containing peptide. The ion at *m/z* 675.1 represents dehydroalanyl GNNSSK, which is formed by β-elimination of the 2,3-dipalmitoyloxypropylthio group. These results prove

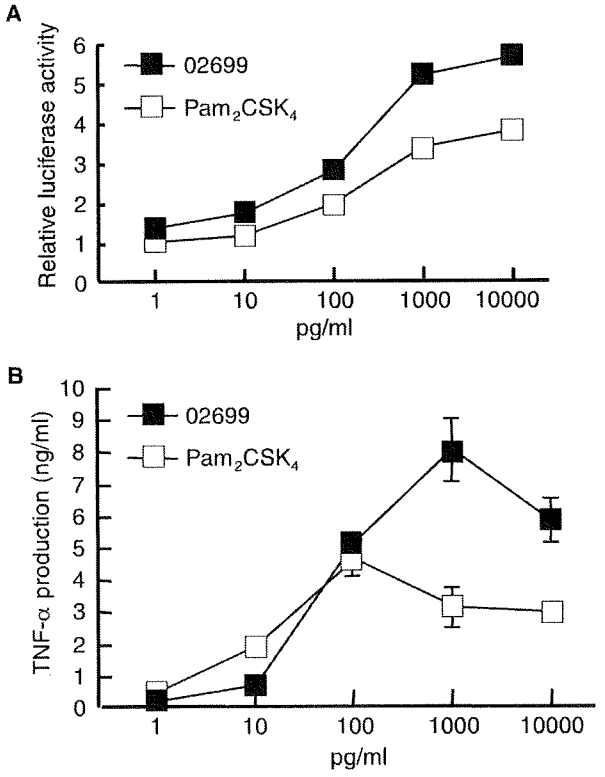

FIGURE 4. **Immunological activities of a synthetic lipopeptide of SAOUHSC_02699.** *A*, NF-κB activation induced by the indicated doses of lipopeptide in Ba/mTLR2 cells for 4 h was measured with a luciferase assay. The results are shown as relative luciferase activity, which was determined as the ratio of stimulated to nonstimulated activity. The data represent the mean ± S.E. obtained from three independent experiments. *B*, TNF-α production induced by the lipoprotein in human PBMC. The levels of TNF-α in the culture supernatants of the cells incubated with the indicated concentration of the stimuli for 4 h were measured by enzyme-linked immunosorbent assay. The data represent the mean ± S.E. obtained from three independent experiments.

that the N-terminal structure of SAOUHSC_02699 is a diacyl-type lipoprotein. The synthetic counterpart of its N-terminal lipopeptide 10-mer stimulated TLR2-dependent NF-κB activation in Ba/mTLR2 cells and TNF-α induction in PBMC (Fig. 4). The lipoprotein SAOUHSC_00634 and -02650 were also subjected to the phase transfer surfactant-aided trypsin digestion. Although active components were eluted from HPLC, no spectra corresponding to lipopeptide were obtained, suggesting that further improvement is required for complete digestion of some lipoproteins.

DISCUSSION

S. aureus is known to activate TLR2, but the principal molecule responsible for this activity has not been proven. In this study, we identified several lipoproteins including SAOUHSC_01002, -01180, -02554, -00634, -02650, -00844, and -02699 as candidates of TLR2-activating molecules (Fig. 1*C*). Some of the lipoproteins were identified as quinol oxidase (SAOUHSC_01002), and the ATP-binding cassette transporter (SAOUHSC_02699, SAOUHSC_00634) and the others were classified as hypothetical proteins. SAOUHSC_00634 has been previously reported as SitC, which acts as an iron-regulated ATP-binding cassette transporter in *S. aureus* and *Staphylococcus epidermidis* and is a major lipoprotein that is distributed throughout the cell wall (26). SAOUHSC_00634 and -01180 were also identified in the membrane fraction of *S. aureus* (13). Although some of lipoproteins reported (13) were not identified in our study, probably because of differences in the culture conditions, similar lipoproteins were extracted. Thus, we consider lipoproteins to be constitutively expressed in *S. aureus*.

SAOUHSC_02699, -02650, and -00634, which were separated by preparative SDS-PAGE (Fig. 2*A*), activate TLR2-expressing cells (Ba/mTLR2) but not murine TLR4- and MD-2-expressing Ba/mTLR4/mMD-2 cells or the negative control Ba/κB cells (Fig. 2*B*). They also exert strong TNF-α-inducing activity on murine and human immune cells (Fig. 2, *D* and *E*). These data indicate that the lipoproteins are the TLR2-activating ligands in *S. aureus*. Sa-M-TX contained LTA, which was visualized in the range of 15–23 kDa (Fig. 1*B*), whereas the activity of Sa-M-TX was observed in the range of 30–35 kDa (Fig. 1*B*). We have previously reported that the LTA fraction derived from an *S. aureus* lipoprotein knock-out mutant is 100-fold less potent than that of the wild-type (15). Although the LTA is still thought to be a TLR2-activating molecule (27), the principal molecules responsible for the TLR2 activity of Sa-M-TX are concluded to be lipoproteins.

Because the three lipoproteins separated were predominant constituents in Sa-M-TX and the sum of their activities is comparable with that of Sa-M-TX (Figs. 1*A* and 2*B*), they are responsible for most of the activity in Sa-M-TX. As for the TLR2-mediated recognition of whole *S. aureus*, it should include other lipoproteins, which depend on the condition of bacteria. Characterization of lipoproteins expressed in a pathogenic condition is important for the analysis of virulence factors by *S. aureus* in infectious diseases.

In the case of Gram-negative bacteria and mycoplasma, several lipoproteins have been identified as TLR2 ligands, and their N-terminal lipopeptides, which contain diacylated or triacylated *S*-(2,3-dihydroxypropyl)cystein, have been proven to be essential moieties for TLR2 activity using chemically synthesized compounds. Lipoproteins derived from Gram-negative bacteria, such as *E. coli, Borrelia burgdorferi, Neisseria gonorrhoeae,* and *Porphyromonas gingivalis,* have been proven to be triacylated lipoproteins (28–31). Mycoplasma, such as *Mycoplasma fermentans* and *Mycoplasma salivarium,* have been shown to possess diacylated lipoproteins (32, 33). However, it is not clear whether the lipoproteins in Gram-positive bacteria are diacylated or triacylated. In this study, we identified the N-terminal structure of *S. aureus* lipoprotein SAOUHSC_02699 as diacylated lipoproteins (Fig. 3). We also confirmed its activity using a synthetic counterpart (Fig. 4). In several bacteria, but not all, the N terminus of the diacylglyceryl-modified cysteine residue is fatty-acylated by a lipoprotein *N*-acyltransferase (*lnt*) (34). Stoll *et al.* (13) screened the published genome sequences of *S. aureus* strains for a gene encoding an *lnt* homolog and found no such protein. These data correspond to our data that the lipoproteins in *S. aureus* are diacylated.

Kurokawa *et al.* (35) recently reported that N terminus of *S. aureus* SitC lipoprotein is triacylated. They also suggested the existence of another type of *N*-acyltransferase distinct from *lnt*. Although the results did not agree with our analytical data, it is possible to consider that strain variation or cultural condi-

tion may affect the activity of the suggested enzyme. Further analysis must be necessary.

In conclusion, we identified TLR2-activating lipoproteins from *S. aureus* cells and characterized the N-terminal lipopeptide structure of a lipoprotein SAUOHSC_02699 as a diacylated one. Because these lipoproteins are considered to contribute to the virulence of *S. aureus*, further studies using protein expression or organic synthetic chemistry are now ongoing to clarify their immunobiological properties.

Acknowledgments—We thank Professor Kazuhisa Sugimura at Kagoshima University for measuring luciferase activity.

REFERENCES

1. Lowy, F. D. (1998) *N. Engl. J. Med.* **339,** 520–532
2. Takeuchi, O., Hoshino, K., Kawai, T., Sanjo, H., Takada, H., Ogawa, T., Takeda, K., and Akira, S. (1999) *Immunity* **11,** 443–451
3. Schwandner, R., Dziarski, R., Wesche, H., Rothe, M., and Kirschning, C. J. (1999) *J. Biol. Chem.* **274,** 17406–17409
4. Travassos, L. H., Girardin, S. E., Philpott, D. J., Blanot, D., Nahori, M. A., Werts, C., and Boneca, I. G. (2004) *EMBO Rep.* **5,** 1000–1006
5. Inohara, N., Ogura, Y., Fontalba, A., Gutierrez, O. Pons, F., Crespo, J., Fukase, K., Inamura, S., Kusumoto, S., Hashimoto, M., Foster, J. S., Moran, P. A., Fernandez-Luna, L. J., and Nuñez, G. (2003) *J. Biol. Chem.* **278,** 5509–5512
6. Chamaillard, M., Hashimoto, M., Horie, Y., Masumoto, J., Qiu, S., Saab, L., Ogura, Y., Kawasaki, A., Fukase, K., Kusumoto, S., Valvano, M. A., Foster, S. J., Mak, T. W., Nuñez, G., and Inohara, N. (2003) *Nat. Immunol.* **4,** 702–707
7. Morath, S., Geyer, A., and Hartung, T. (2001) *J. Exp. Med.* **193,** 393–397
8. Suda, Y., Tochio, H., Kawano, K., Takada, H., Yoshida, T., Kotani, S., and Kusumoto, S. (1995) *FEMS Immunol. Med. Microbiol.* **12,** 97–112
9. Hashimoto, M., Yasuoka, J., Suda, Y., Takada, H., Yoshida, T., Kotani, S., and Kusumoto, S. (1997) *J. Biochem.* **121,** 779–786
10. Han, S. H., Kim, J. H., Martin, M., Michalek, S. M., Nahm, M. H. (2003) *Infect. Immun.* **71,** 5541–5548
11. Hashimoto, M., Imamura, Y., Morichika, T., Arimoto, K., Takeuchi, O., Takeda, K., Akira, S., Aoyama, K., Tamura, T., Kotani, S., Suda, Y., and Kusumoto, S. (2000) *Biochem. Biophys. Res. Commun.* **273,** 164–169
12. Hashimoto, M., Tawaratsumida, K., Kariya, H., Aoyama, A., Tamura, T., and Suda, Y. (2006) *Int. Immunol.* **18,** 355–362
13. Stoll, H., Dengjel, J., Nerz, C., and Götz, F. (2005) *Infect. Immun.* **73,** 2411–2423
14. Bubeck, J. W., Williams, W. A., and Missiakas, D. (2006) *Proc. Natl. Acad. Sci. U. S. A.* **103,** 13831–13836
15. Hashimoto, M., Tawaratsumida, K., Kariya, H., Kiyohara, A., Suda, Y., Krikae, F., Kirikae, T., and Götz, F. (2006) *J. Immunol.* **177,** 3162–3169
16. Iordanescu, S., and Surdeanu, M. (1976) *J. Gen. Microbiol.* **96,** 277–281
17. Shibata, K., Hasebe, A., Sasaki, T., and Watanabe, T. (1997) *FEMS Immunol. Med. Microbiol.* **19,** 275–283
18. Hirschfeld, M., Ma, Y. Weis, J. H., Vogel, S. N., and Weis, J. J. (2000) *J. Immunol.* **165,** 618–622
19. Laemmli, U. K. (1970) *Nature* **227,** 680–685
20. Wallis, R. S., Amir-Tahmasseb, M., and Ellner, J. J. (1990) *Proc. Natl. Acad. Sci. U. S. A.* **87,** 3348–3352
21. Towbin, H., Staehelin, T., and Gordon, J. (1979) *Proc. Natl. Acad. Sci. U. S. A.* **76,** 4350–4354
22. Jensen, O. N., Wilm, M., Shevchenko, A., and Mann, M. (1999) *Methods Mol. Biol.* **112,** 513–530
23. Perkins, D. N., Pappin, D. J., Creasy, D. M., and Cottrell, J. S. (1999) *Electrophoresis* **20,** 3551–3567
24. Masuda, T., Tomita, M., and Ishihama, Y. (2007) *J. Proteome Res.* **7,** 731–740
25. Hantke, K., and Braun, V. (1973) *Eur. J. Biochem.* **34,** 284–296
26. Cockayne, A., Hill, J. P., Powell, N. B., Bishop, K., Sims, C., and Williams, P. (1998) *Infect. Immun.* **66,** 3767–3774
27. Schröder, N. W., Morath, S., Alexander, C., Hamann, L., Hartung, T., Zähringer, U., Göbel, B. U., Webe, R., Jr., and Schumann, R. R. (2003) *J. Biol. Chem.* **278,** 15587–15594
28. Hirschfeld, M., Kirschning, C. J., Schwandner, R., Wesche, H., Weis, J. H., Wooten, R. M., and Weis, J. J. (1999) *J. Immunol.* **163,** 2382–2386
29. Lee, H. K., Lee, J., and Tobias, S. P. (2002) *16 J. Immunol.* **8,** 4007–4012
30. Fisette, P. L., Ram, S., Andersen, M. J., Guo, W., and Ingalls, R. R. (2003) *J. Biol. Chem.* **278,** 46252–46260
31. Hashimoto, M., Asai, Y., and Ogawa, T. (2004) *Int. Immunol.* **16,** 431–437
32. Mühlradt, P. F., Kiess, M., Meyer, H., Süssmuth, R., and Jung, G. (1997) *J. Exp. Med.* **185,** 1951–1958
33. Shibata K, Hasebe, A., Into, T., Yamada, M., and Watanabe, T. (2000) *J. Immunol.* **165,** 6538–6544
34. Sankaran, K., and Wu, H. C. (1994) *J. Biol. Chem.* **269,** 19701–19706
35. Kurokawa, K., Lee, H., Roh, K-B., Asanuma, M., Kim, Y. S., Nakayama, H., Shiratsuchi, A., Choi, Y., Takeuchi, O., Kang, H. J., Dohmae, N., Nakanishi, Y., Akira, S., Sekimizu, K., and Lee, B. L. (January 12, 2009) *J. Biol. Chem.* 10.1074/jbc.M809618200

J. Biochem. 2009;145(6)799–810
doi:10.1093/jb/mvp039

Effective Induction of Cell Death on Adult T-Cell Leukaemia Cells by HLA-DRβ-Specific Small Antibody Fragment Isolated from Human Antibody Phage Library

Satoshi Muraoka[1], Yuji Ito[1,*], Masaki Kamimura[1], Masanori Baba[2], Naomichi Arima[2], Yasuo Suda[3], Shuhei Hashiguchi[1], Masaharu Torikai[4], Toshihiro Nakashima[4] and Kazuhisa Sugimura[1]

[1]Department of Bioengineering, Faculty of Engineering, Kagoshima University, Korimoto 1-21-40, Kagoshima, Kagoshima 890-0065; [2]Center for Chronic Viral Diseases, Graduate School of Medical and Dental Sciences, Kagoshima University, Sakuragaoka 8-35-1, Kagoshima, Kagoshima 890-8544; [3]Nanostructured and Advanced Materials Course, Graduate School of Science and Engineering, Kagoshima University, Korimoto 1-21-40, Kagoshima, Kagoshima 890-0065; and [4]The Chemo-Sero-Therapeutic Research Institute, Kyokushi, Kikuchi, Kumamoto 869-1298, Japan

Received December 19, 2008; accepted February 23, 2009; published online March 6, 2009

By a biopanning method using cell sorter, we quickly isolated an antibody phage clone (S1T-A3) specific to human T-lymphotropic virus type 1-carrying T-cell line S1T from a human single chain Fv (scFv) antibody phage library. This scFv antibody bound to HTLV-1-carrying T-cell lines including MT-2, MT-4 and M8166 other than S1T, but not to non-HTLV-1-carrying T-cell lymphomas such as Jurkat and MOLT4 cells. Interestingly, this antibody induced the cell death on S1T cells very quickly (<30 min). We tried to identify the target molecules by western blotting and mass spectrometric analysis, revealing that the target antigen was HLA class II DR. The cell death was induced only in dimmer form of scFv (diabody) and at 15-fold lower concentration than that of a fusion protein of scFv and human IgG Fc [$(scFv)_2$-Fc] or anti HLA-DR mouse whole antibody L243. Thus, S1T-A3 diabody is a small antibody fragment with agonistic activity to induce cell death through HLA-DR. This is the first report elucidating that diabody specific to HLA-DR is effective to induce the cell death in T-cell malignancy especially adult T-cell leukaemic cell line.

Key words: adult T-cell leukaemia, human antibody, scFv, phage library, diabody.

Abbreviations: APC, antigen presenting cells; ATL, adult T-cell leukaemia; FACS, fluorescence-activated cell sorter; FBS, fetal bovine serum; FITC, fluorescent isothiocyanate; HLA, human leucocyte antigen; HTLV-1, human T-cell leukaemia virus type 1; mAb, monoclonal antibody; MHC, major histocompatibility complex; PE, phycoerythrin; PI, propidium iodide; RMF, relative mean fluorescence; scFv, single chain Fv; SPR, surface plasmon resonance.

ATL (adult T-cell leukaemia) is a disease, which is caused by infection of the retrovirus HTLV-1 (human T-cell leukaemia virus type 1) to $CD4^+$ T cells. As many as 10–20 million people worldwide are estimated to carry the virus (*1*, *2*). Other diseases caused by HTLV-1 infection include HAU (HTLV-1 associated uveitis) and HAM/TSP (HTLV-1-associated myelopathy/tropical spastic paraparesis), which is a neuro-degenerative disease. Although the frequency of ATL development in the life of the carriers is low (2–6%), its prognosis is generally severe after the development of ATL (*2*). Nevertheless, a human antibody for therapeutic use of ATL has not yet been established until now.

The antibody phage library has become a major technology that directly isolates human antibodies for therapeutic use (*3*), along with hybridoma technology using trans-chromosome mouse (*4*). In cell panning to isolate the cell-specific phages by antibody phage display library, several methods were developed to remove non-specific phages, for example, by washing the cells with repeating centrifugation and suspension (*5*), by recovering the cells with magnet beads (*6*) or by sedimentation of the cells though centrifugation in organic solvent (*7*). We employed here another panning method using cell sorter (*8*, *9*) for rapid isolation of the binders and for less damage giving the cells. Furthermore, by use of the control cells as absorber, we could obtain the antibody phages which recognize the unique antigens expressed specifically on the target cells, facilitating the finding of novel tumour markers (*10*, *11*).

We isolated a human scFv antibody specific to S1T cells, a cell line derived from an ATL patient (*12*) by a cell panning method using a cell sorter from a single chain Fv (scFv) human antibody phage library. Interestingly, the obtained scFv antibody induced a cell death on S1T cells within in a very short time (<30 min). In this report, we identified the antigen on S1T cells targeted by this scFv and elucidated the molecular structures which is essential for inducing the cell death. The antibody isolated here can be expected as small therapeutic antibody to kill the malignant T cells.

*To whom correspondence should be addressed. Tel: +81-99-285-8346, Fax: +81-99-285-8346, E-mail: yito@be.kagoshima-u.ac.jp

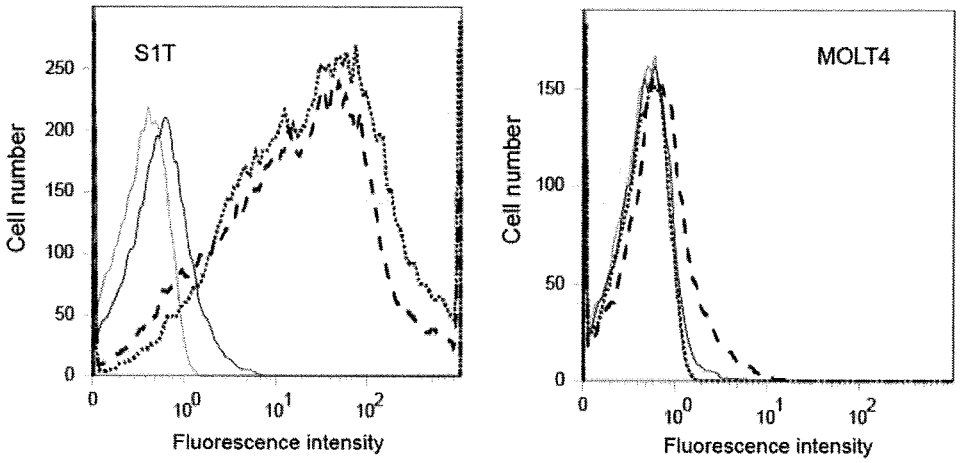

Fig. 1. **The enrichment of the S1T cell-specific phages by cell panning on cell sorter.** The binding activities of the phages amplified after each round of cell panning against S1T cells were analysed using FACS. The lines represent the histograms after the first (thick line), second (broken line) and third round (dotted line) of cell panning. The grey line indicates the control data of the cells stained without phages.

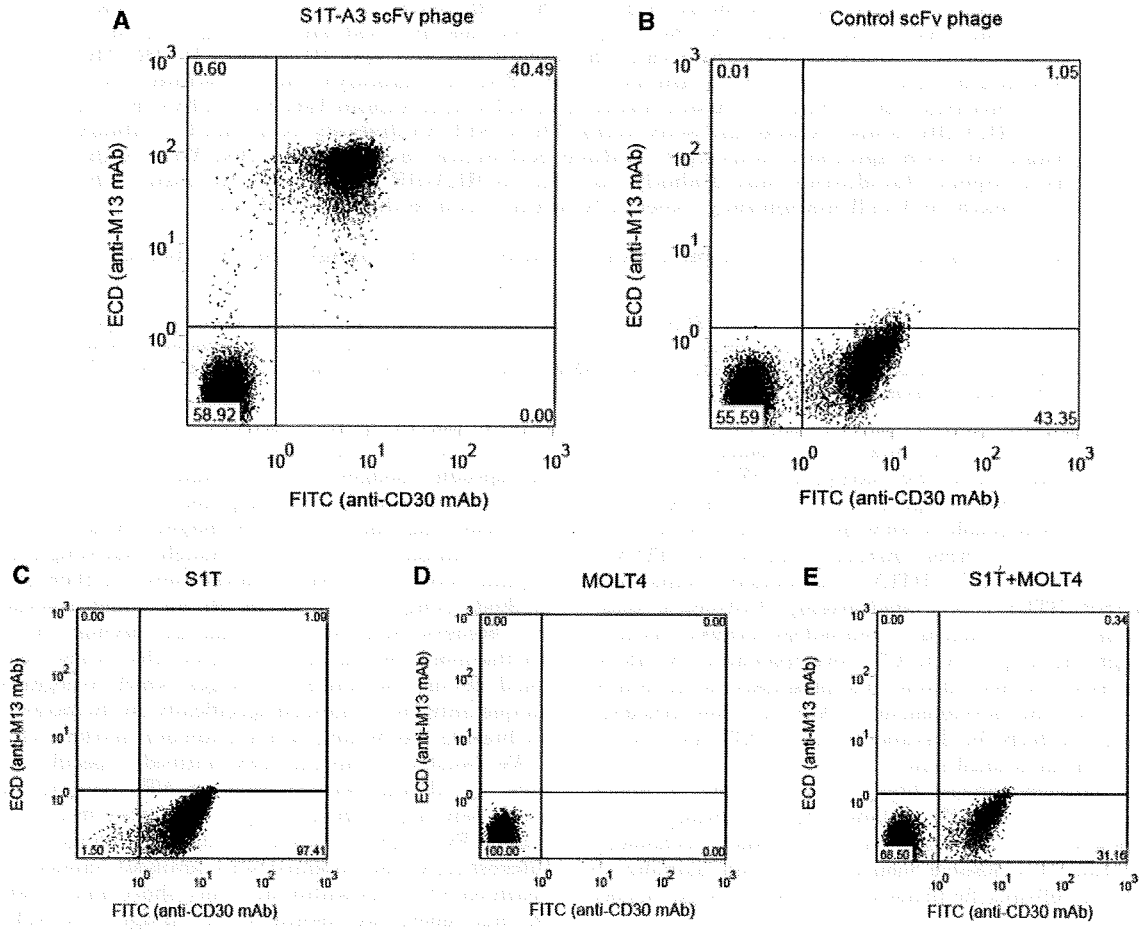

Fig. 2. **The binding specificity of S1T-A3 phage clone to S1T cell.** S1T-A3 (A) or non-specific control (B) phages were incubated with the mixture of MOLT4 and S1T cells, the latter of which were labelled with FITC-conjugated anti CD30 mAb, and analysed on FACS. The other three panels indicate the FACS data for S1T cells labelled with FITC-conjugated anti CD30 mAb (C), non-labelled MOLT4 cells (D) and their mixture (E), respectively.

(a) Amino acid sequence of the VH domain

```
                FLR1                            CDR1            FLR2                    CDR2
EVQLLQSGGGLVQPGRSLRLSCAASGFTFD DYAMH WVRQAPGKGLEWVS GISWNGGNIDYADSVRG

                FLR3                            CDR3            FLR4
RFTISRDNAKNSLYLQMDSLRAEDTALYYCAK APGMLIYYSYMDV WGKGTMVTVSS
```

(b) Amino acid sequence of the VL domain

```
            FLR1                    CDR1            FLR2            CDR2
QPVLTQPPSVSVSPGQTARITC SGDRLPRQYVY WYQQKPGQAPVLLIY KDIERPS

            FLR3                            CDR3        FLR4
GIPERFSGSTSGTTVTLTINGVQAEDEADYSC QSADSSETYPV FGGGTK VTVLGAAA
```

(c) Variable gene usage

	Heavy chain			Light chain	
clone	V	D	J	V	J
S1T-A3	IGHV3-9*01	IGHD3-3*01	IGHJ6*03	IGLV3-25*03	IGLJ3*02

Fig. 3. **The amino acid sequence of the S1T-A3 scFv clone deduced from the DNA sequence.** The complementary determining regions (CDR1–CDR3) and the frame regions (FR1–4) were assigned according to Kabat's numbering. The CDR regions are indicated in bold letters (A and B). The scFv nucleotide sequence was analysed by searching the IMGT/V-QUEST database to identify the gene usage on the immunoglobulin germ line (C) (*35*).

MATERIALS AND METHODS

Cells and Proteins—The HTLV-1-carrying T-cell line S1T was previously established from the peripheral blood mononuclear cells (PBMCs) of an ATL patient (*12*). The other cells used here (HTLV-1-carring T-cell lines: MT-2, MT-4 and M8166; HTLV-1-negative T-cell lymphoma cell lines: MOLT-4 and Jurkat; B-cell lymphoma cell lines: Dauji and Raji) are described in the previous report (*13*). All cell lines were maintained in RPMI 1640 medium supplemented with 10% heat-inactivated fetal bovine serum (FBS), 100 U/ml penicillin G and 100 μg/ml streptomycin. The murine L929 cells (ATCC CCL-1) transfected with the human HLA-DR genes (HLA-DRB*0101 and HLA-DRA*0101) are referred to as L57.23 cells. The purified HLA-DR molecule (DRA*0101/DRB1*0405) was kindly gifted by Prof. S. Matsushita (*10*).

Antibody Phage Library—Human naive scFv phage library with a diversity of 4.5×10^8 was constructed using pCANTAB5E phagemid vector, as described previously (*14*).

Cell Panning on Flow Cytometry—One million S1T cells were labelled with fluorescent isothiocyanate (FITC)-conjugated anti-human CD30 mouse monoclonal antibody (mAb) for 30 min on ice and were washed once with phosphate-buffered saline (PBS). After adding 1×10^6 MOLT4 cells, the cells were suspended in 500 μl PBS containing 1% BSA and were incubated with the scFv-phage library of 1×10^{12} TU (transforming unit) at 4°C for 1 h, with gentle shaking on a rotator. After centrifugation (500*g*, 30 s), the cells were re-suspended in PBS containing 2% FBS (2.5×10^5 cells/ml in 8 ml). After filtration through 40 μm Nylon Mech (Kyoshin Rikoh Inc.), the cells were supplied for cell sorting on an EPICS ALTRA HyperSort (Beckman coulter Inc.) with fluorescence emission (512 nm) by excitation at 488 nm. The S1T cells separated by cell sorting were suspended in PBS and treated with 76 mM citric acid solution (pH 2.5) at room temperature for 5 min to dissociate the bound phages. After neutralization with 1 M Tris–HCl (pH 7.4), the cell suspension was transferred to the culture of *Escherichia coli* TG1 in logarithmic growth phase for infection. The scFv-displayed phages were rescued by co-infection with M13KO7 helper phage and purified by polyethylene glycol (PEG) precipitation from the culture supernatant, as described previously (*14*, *15*). This biopanning process was repeated three times. The phages after the second and third round of biopanning were cloned and used for binding analysis on flow cytometry.

Flow Cytometric Analysis—The mammalian cells with 80–90% confluent growth were collected by centrifugation and washed once in cold PBS and twice in FACS buffer (PBS containing 10% FBS and 0.1% sodium azide). The cells (1×10^6 cells) were incubated with the cloned phages or the purified scFv for 30 min. After washing the cells twice with FACS buffer, the phages bound to cells were stained by biotinylated anti-M13 mAb (GE Healthcare) and phycoerythrin (PE)-conjugated

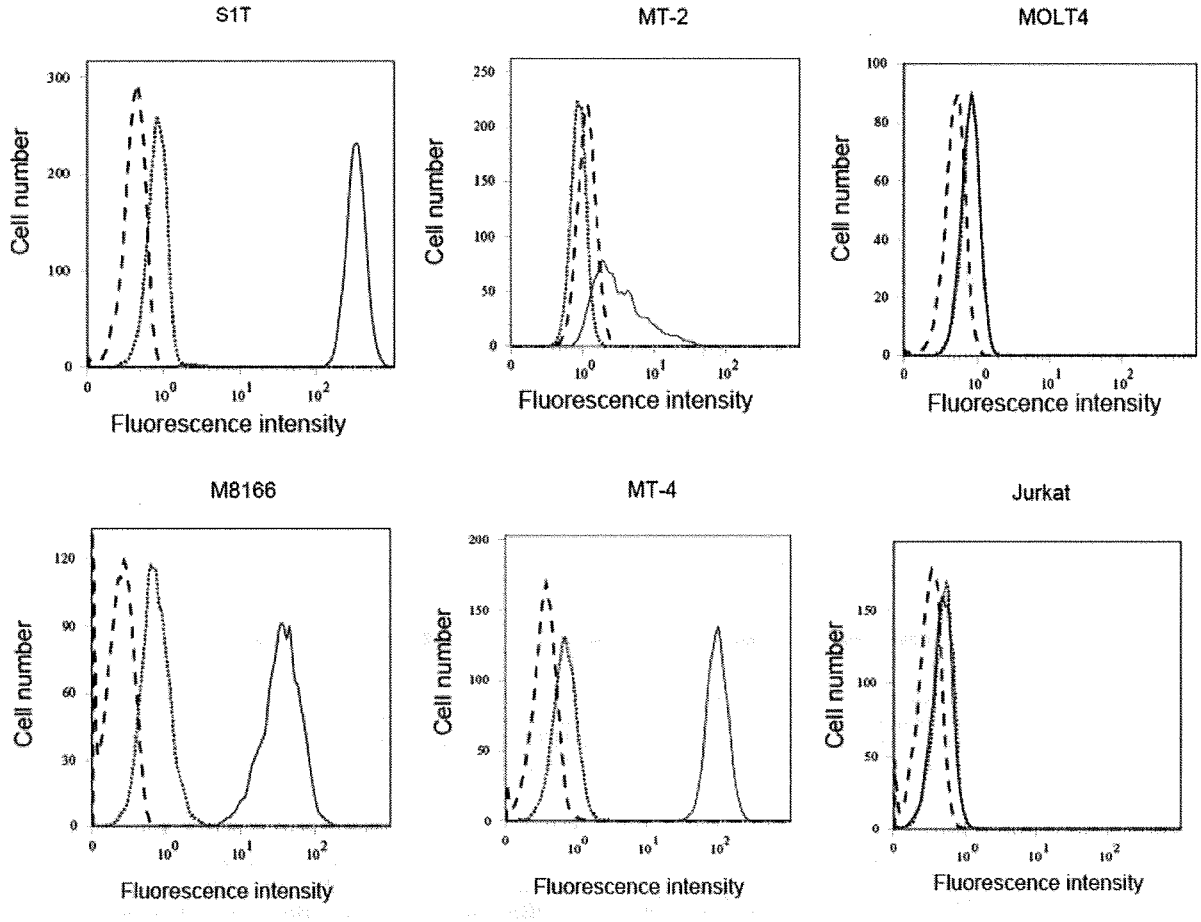

Fig. 4. **Bindings of S1T-A3 scFv to HTLV-1-carrying T-cell lines (S1T, MT-2, MT-4 and M8166) and non-HTLV-1-carrying T-cell lines (MOLT4 and Jurkat).** The cells were stained with scFv, anti-His-tagged mouse mAb and FITC-labelled anti mouse antibody and supplied to FACS analysis (thick line). The broken and dotted lines indicate the cells only and the cells stained without scFv, respectively. The increase of the fluorescence intensity of the cells by binding with scFv was evaluated as the relative mean fluorescence (RMF) with scFv *vs.* without scFv, which gave the values of 330, 116, 51, 3.0, 1.1, 1.2 for S1T, MT-4, M8166, MT-2, MOLT4 and Jurkat cells, respectively.

streptavidin (Beckman Coulter Inc.). The scFv that bound to the cells was stained with an anti-His tag mAb (GE Healthcare) and FITC-conjugated anti-mouse IgG antibody. For staining HLA-DR, PE-conjugated anti-HLA-DR (L243) mAb was used. Cells were washed twice with FACS buffer and then analysed on an EPICS XL flow cytometer (Beckman Coulter Inc.).

Purification of scFv for Cellular Assay—The expression of scFv in *E. coli* HB2151 infected with the phage clone S1T was localized in the cytoplasmic fraction. Therefore, the original C-terminal tag (E-tag) of scFv was replaced with a His-tag by recombination of the gene from pCANTAB5E to a pCANTAB6 vector to generate pCANTAB6/S1T-A3 phage. The phage was infected to *E. coli* HB2151 and the S1T-A3 scFv was expressed in HB2151 by induction of 1 mM IPTG at 30°C. The bacterial cells were disrupted by ultrasonication and the supernatant obtained by centrifugation was supplied to affinity purification on His Trap^{TM}HP column (GE Healthcare), according to the manufacturer's instructions. The scFv was further purified on the gel permeation HPLC on Superdex75 (10/300 GL, GE Healthcare) equilibrated with 0.1 M phosphate buffer (pH 7.0).

Mass Spectrometric Analysis for Antigen Determination—The S1T cells were lysed in lysis buffer (pH 7.4, 10 mM Tris–HCl buffer containing 0.5 mM EDTA, 150 mM NaCl, 1% Tween-20, 50 μg/ml DNase I and protein inhibitor cocktail, Sigma–Aldrich) by combination with the ultrasonic disintegrator. The cell lysate was centrifuged and the supernatant was mixed with 2 × SDS sample buffer containing 5% 2-mercaptethanol and subjected to SDS–PAGE on 5–20% gradient gel. The gel was subsequently supplied to western blot analysis to detect the protein band, which was recognized by S1T-A3 scFv. After CBB-staining, the gel fragment including the positive band on western blot was excised, destained and in-gel digested with trypsin. The digested peptides were analysed on LC-MS/MS (Medigenomics, Germany) and their mass spectrum data were analysed by MASCOT search.

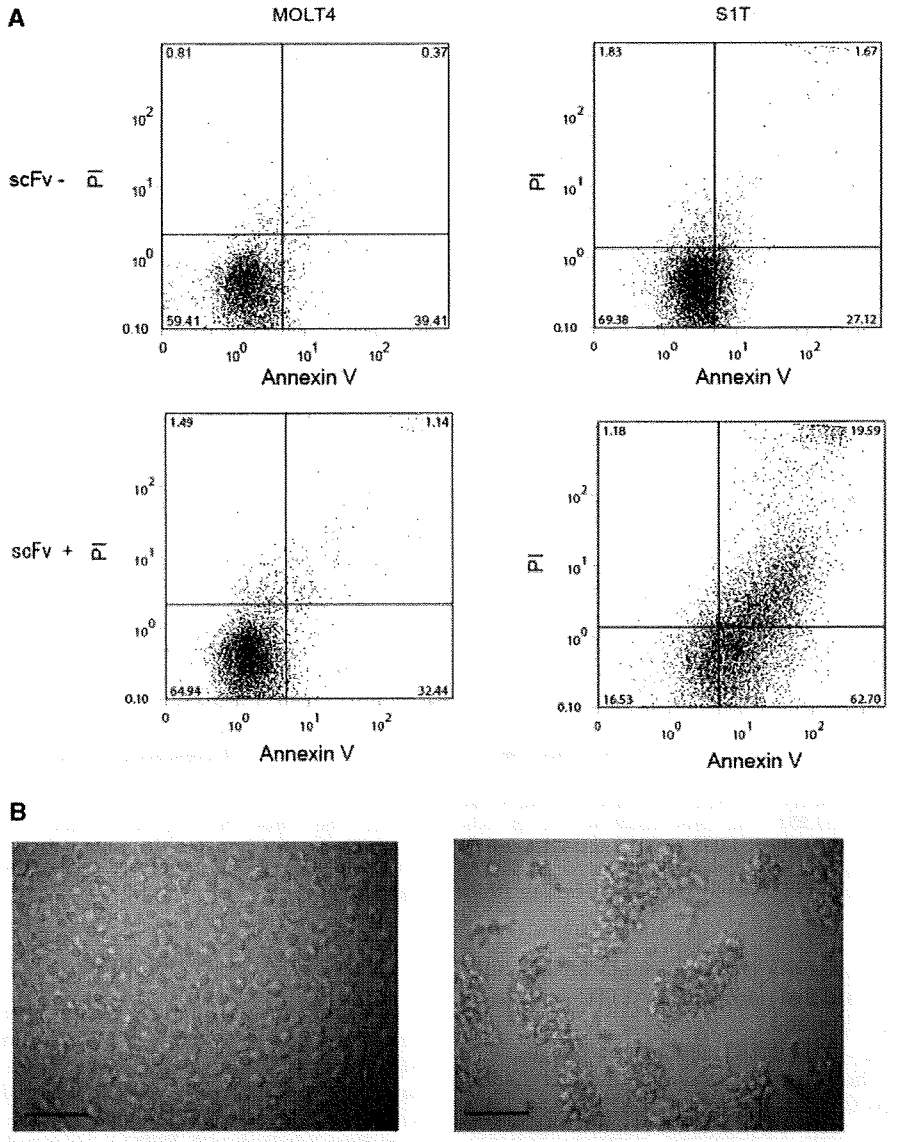

Fig. 5. **Cell death of S1T cells induced by S1T-A3 scFv.** (A) S1T cells or MOLT4 cells were incubated with S1T-A3 scFv (5 nM) at 37°C for 1 h and were stained with propidium iodide (PI) and Annexin V staining solution for 15 min. The stained cells were analysed on a flow cytomer. (B) Morphological aspects of the cell death were examined on OLYMPUS IX71 microscope. The S1T cells were incubated with 10 nM scFv (right panel) or with no scFv (left panel) for 30 min and subjected to the microscopic observation. Scale bar in picture indicates the length of 200 μm.

Preparation of $(scFv)_2$-Fc of SIT-A3—ScFv gene of SIT-A3 was cloned into mammalian expression vector pCAG-H with a human IgG_1 constant region (*16*, pCAG-H- SIT-A3). $(ScFv)_2$-Fc of SIT-A3 was expressed by using FreeStyle 293 system (Invitrogen). Briefly, FreeStyle 293 cells were transfected with a pCAG-H-SIT-A3 by 293 fectin according to the manufacturer's instruction and culture 72 h. The supernatants were removed from the cells by centrifugation and filtered through a 0.22-μm membrane. The expressed $(scFv)_2$-Fc of SIT-A3 was purified by protein A affinity chromatography (GE healthcare). Purified $(scFv)_2$-Fc of SIT-A3 was analysed by size-exclusion chromatography under presence of 0.2 M arginine (*17*).

Cell Killing and Apoptosis Assay—Cells (1×10^5 cell/30 μl) in RPMI 1640 medium containing 10% FBS were incubated with anti-HLA-DR antibodies at 37°C for 30 min. The cells were centrifuged and subjected to the flow cytometer to count the viable cells. The killing activity (%) was evaluated by viable cell recovery: [(viable untreated)–(viable treated)]/(viable untreated) × 100. The Annexin V-FITC assay was also performed

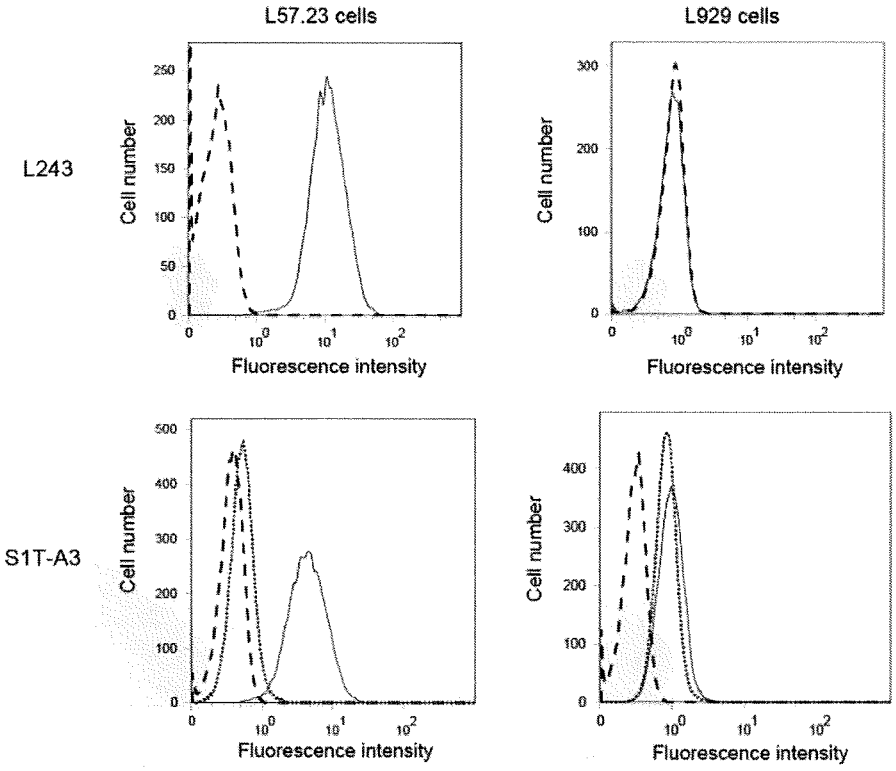

Fig. 6. **Binding specificity of S1T-A3 scFv to HLA-DR-expressing L cells (L57.23).** The cells (L929 or L57.23 cells) were stained with PE-labelled L243 mAb (anti-HLA-αchain mouse mAb, thick line in the upper panel) or with S1T-A3 scFv, anti-His mAb and FITC-labelled anti-mouse mAb (thick line in the lower panel). The dotted lines in the lower panel indicate the data for staining without scFv. The broken lines indicate the data for the cells only. The RMF values of S1T-A3 binding were 9.2 and 1.3 for L57.23 cells and L cells, respectively.

to quantitatively determine the percentage of apoptotic cells using the TACSTM Annexin V-FITC apoptosis detection kit (R&D System).

DNA Sequencing—The DNA sequence of phages was determined by the Dye Terminator method using primer1 (5′-CAACGTGAAAAAATTATTATTCGC-3′ for scFv gene) on the ABI PRISM3100 Genetic Analyzer (Applied Biosystems, Foster City, CA, USA)

ELISA—Each well of the microplate (Nunc, Maxisop) was coated with HLA-DR (50 ng/40 μl/well) in 0.1 M $NaHCO_3$ and blocked with 0.5% BSA in PBS. scFv was added to each well and incubated for 1 h. The wells were washed five times with PBS containing 0.1% Tween-20 and the bound scFv was detected by an anti-His tagged mouse mAb and alkaline-phosphatase (AP)-conjugated anti-mouse IgG (Jackson Immuno Research, West Grove, PA, USA). Using p-nitrophenyl phosphate as a substrate, the colorimetric assay was performed measuring the absorbance at 405 nm using a microplate reader NJ-2300 (System Instruments, Tokyo)

Protein Concentrations—Protein concentrations were determined from the absorbance at 280 nm using molecular extinction coefficients (ε_{280}) of 48,360, 96,720 and 167,400 (absorbance unit of $M^{-1}cm^{-1}$) for scFv monomer, diabody and $(scFv)_2$-Fc, respectively.

RESULTS

Isolation of An Antibody Clone Specific to HTLV-1-Carrying Cells—To isolate a human antibody specific to S1T cells (HTLV-1-carring cells) from a human scFv phage library, the cell panning method in combination with a cell sorter were employed. The S1T cells (1×10^6) were first labelled with FITC-conjugated anti-CD30 mAb, as CD30 is known to be highly expressed by adult T-cell leukaemia cell lines (*18*), mixed with control cells (MOLT4, 1×10^6) and reacted with scFv antibody phage library (1×10^{12} TU). The S1T cells were collected by a cell sorter. The phages binding to the cells were amplified through re-infection to *E. coli* TG1 and supplied to the next round of cell panning. After only two rounds of panning, S1T cells-specific binding phages were enriched (Fig. 1). Among the 30 clones isolated from the pooled phages after the second and third rounds of panning, the 15 clones showed the binding activities to the S1T cells. Their DNA sequences were determined and a single clone S1T-A3 was identified. As shown in Fig. 2, S1T-A3 phage indicated the specific binding to S1T cells with no binding to MOLT4 cells, indicating that S1T-A3 recognized a unique antigen expressed on S1T cell. The amino acid sequences of the VH and VL regions of S1T-A3 are shown in Fig. 3.

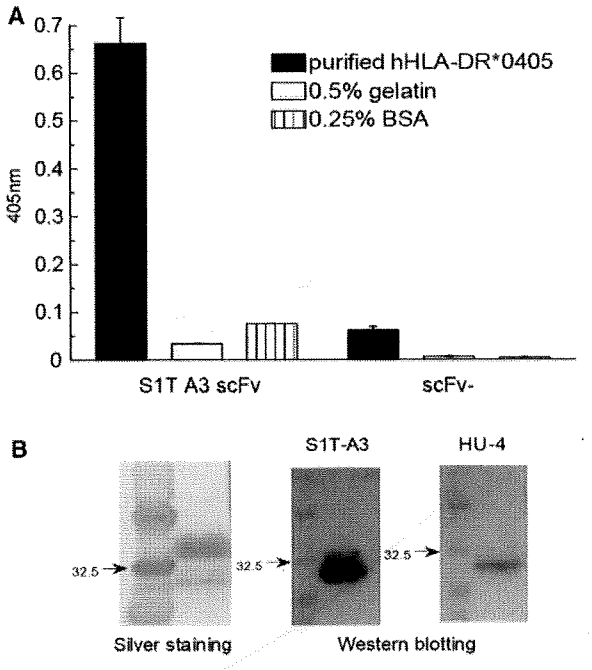

Fig. 7. **Antigen determination of S1T-A3 scFv by ELISA (A) and western blotting (B).** HLA-DR coated on the plate was detected by S1T-A3 scFv, anti-His-tagged mouse mAb and AP-conjugated anti-mouse IgG. The SDS–PAGE gel of HLA-DR was subjected to silver staining or western blot analysis with S1T-A3 scFv or HU-4 mAb (mouse mAb specific to the human HLA-DR β chain). In the silver-stained gel, the upper (34 kDa) and lower (29 kDa) bands corresponded to the HLA-DR α and β chain, respectively.

The scFv was purified from the cytoplasmic fraction of the bacterial cells infected with S1T-A3 phages and the binding analysis was examined against several T cell lymphoma cell lines (HTLV-1-carrying T-cell lines: S1T, MT-2, MT-4 and M8166 and non-HTLV-1-carrying T-cell lines: MOLT4 and Jurkat) on FACS. The results indicated the scFv bound to the four HTLV-1-carring T-cell lines strongly or moderately, but not to the non-HTLV-1-carrying T-cell lines (Fig. 4), suggesting that the cell-surface antigen recognized by S1T-A3 is a potential marker for malignant T-cells during HTLV-1-infection.

Cell-Death-Inducing Activity of S1T-A3 scFv—Of interest, we found that the S1T cells lysed during the incubation with S1T-A3 scFv. Therefore, we examined the apoptotic activity of S1T-A3 by Annexin V/propidium iodide (PI) staining (Fig. 5A). Although apoptosis was generally defined by an increased Annexin V-positive and PI-negative cell population, the S1T cells incubated with S1T-A3 scFv were doubly-stained by PI and Annexin V, suggesting that the cell death induced by S1T-A3 is not typical apoptosis but apoptotic cell death with necrotic properties.

The cell death of S1T cells by S1T-A3 scFv was rapidly induced with 30 min, changing largely the morphology of the cells (Fig. 5B). After incubation of the cells with scFv, the cells were aggregated and lead to cell lysis.

Antigen Targeted by S1T-A3 scFv—We subsequently determined the antigen targeted by S1T-A3 scFv. Western blot analysis of the S1T cell lysate indicated a positive band (32.5 kDa) stained with S1T-A3 scFv (data not shown). The gel fragment corresponding to the positive band on western blot was excised, subjected to in-gel digestion with trypsin and then LC-MS/MS analysis. The mass spectrum data of the obtained peptide fragments were subjected to MASCOT search on human IPI (International Protein Index) database (EMBL-EBI). The potential candidate for antigen of the cell surface was found to be HLA-DRβ.

To confirm this, we examined the binding ability of S1T-A3 scFv to HLA-DR-expressing L57.23 cells, a murine L-cell transfectant with HLA-DRB*0101 and HLA-DRA*0101 genes. S1T-A3 scFv bound to the L57.23 cells but not to control L929 cells (Fig. 6). Furthermore, ELISA and Western blotting analysis using the purified HLA-DR (DRA*0101/DRB1*0405) molecules confirmed the binding of S1T-A3 scFv to HLA-DR and its specificity to β chain of HLA-DR (Fig. 7).

Cell Death Activities Dependent on Molecular Formats of S1T-A3 scFv—Generally, scFv produced by *E. coli* sometimes contains the dimer (diabody) as well as the monomer form. S1T-A3 scFv purified here also contained the two forms of scFv in almost equal amounts, which was detected on the size exclusion chromatography (data not shown). To examine which form is responsible for the cell death activity, each purified scFv form was subjected to cell lysis analysis by counting the viable cells on FACS (Fig. 8). The viable cell number did not change even after treatment with 120 nM scFv monomer. In contrast, the treatment with only 6 nM diabody largely reduced the cell viability to 20%. This finding clearly indicates that the dimer form is essential for the induction of cell death through HLA-DR ligation. This diabody harboured a linker peptide composed of 15 amino acids, $(GGGGS)_3$ between the VH and VL domain. To test the effect of the linker length on cell-death activity, we prepared diabodies with different lengths of linkers composed of $(GGGGS)_2$ and $(GGGGS)_1$, and compared their cell-death activities. The purified three diabodies showed similar dose-dependent activities with EC_{50} of 2–5 nM (data not shown), indicating that the difference of the linker length between 5 and 15 amino acids does not influence the cell death activity so much.

On the other hand, an alternative scFv dimer molecule (a fusion protein of scFv and human IgG Fc, $(scFv)_2$-Fc) was constructed. This molecule showed a comparative binding to S1T cells with a relative mean fluorescence (RMF) of 311 (Fig. 9A), where that of S1T-A3 scFv was 330 (Fig. 4). The surface plasmon resonance (SPR) analysis on BIAcore also showed a tight binding of $(scFv)_2$-Fc to HLA-DR molecules with an apparent dissociation constant K_d of 1.9 nM (Fig. 9B). In spite of its tight binding, $(scFv)_2$-Fc unexpectedly showed a weak cell death-inducing activity (EC_{50}: 26 nM ± 8), which was 15-fold more than that of the diabody (EC_{50}: 1.8 nM ± 0.8) and similar to that of L243 mAb (EC_{50}: 22 nM ± 2), an apoptosis-inducing mouse mAb specific to α chain of HLA-DR.

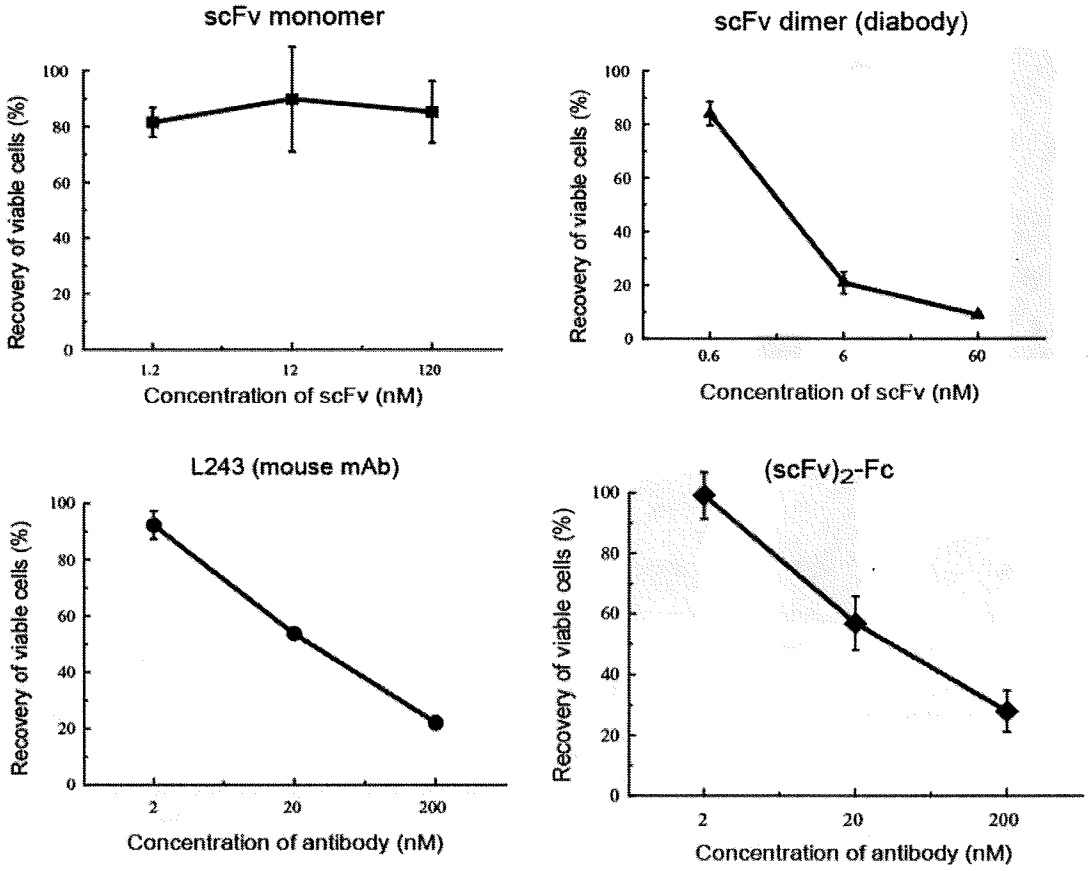

Fig. 8. **Cell-death-inducing activities by the different molecular forms of S1T-A3 scFv [monomer, diabody and $(scFv)_2$-Fc] on S1T cells.** The S1T cells were treated with the different forms of scFv at the indicated concentrations. The viral cells were recovered by centrifugation and were counted using the flow cytometer. The recovery yields of the cells are expressed as a percent ratio of the cell count with *vs.* without the antibody treatment. The L243 mouse mAb was used as a control Ab inducing cell death.

Cell-Death-Inducing Activities of S1T-A3 Diabody on Other HLA-DR Expressing Cells—We further examined the cell-death-inducing activities of S1T-A3 diabody on the cell lines other than S1T cells (Fig. 10A). Under the condition where more than 90% S1T cells died, the cell death was observed in 60% of MT-4, 8% of M8166 and 15% of Daudi cells, and the no significant cell death was done in MOLT4 cells. These cell-death capabilities seem to accord with the expression level of HLA-DR on the surface of the cells. Figure 10B showed the expression level of HLA-DR examined on FACS by staining with anti-HLA-DR α chain mouse mAb (L243). The S1T cells highly expressed HLA (RMF: 520), MT-4 or Daudi cells moderately (RMF: 72, 55). M8166 and MOLT4 cells at very low level or not at all (RMF: 4.0 and 1.0). Interestingly, in spite of the similar expression of HLA (RMF:72 and 55) and the comparable cell-death induction by L243 mAb (14 and 20%) between MT-4 and Daudi cells, the extent of the cell death by S1T-A3 diabody was largely different (15% and 60% for MT-4 and Daudi). This discrepancy may be caused by the differences of the accessory molecules for HLA-derived cell-death signalling and/or of HLA β chain isoforms between the cell lines.

DISCUSSION

In this report, we identified HLA-II molecules as a S1T cell-specific marker by isolation of S1T-specific antibody (scFv) and determination of its antigen. HLA-II (human MHC-class II molecules) is a heterodimer composed of an α chain and a highly variable β chain, and classified into three groups of the gene family, namely HLA-DP, HLA-DQ and HLA-DR. This molecule is expressed on the antigen presenting cells (APC) such as macrophages and dendritic cells, and functions as antigen presentation molecule to T cells in the activation of the immune response (*19, 20*). It is well known that the expression of these molecules is increased in the malignant lymphomas and therefore especially HLA-DR has become a clinical target for antibody therapy to B-cell lymphoma (*21, 22*). On the other hand, it was reported that HLA-DR expression is enhanced in the activated T-cells or in malignant T-cells including several

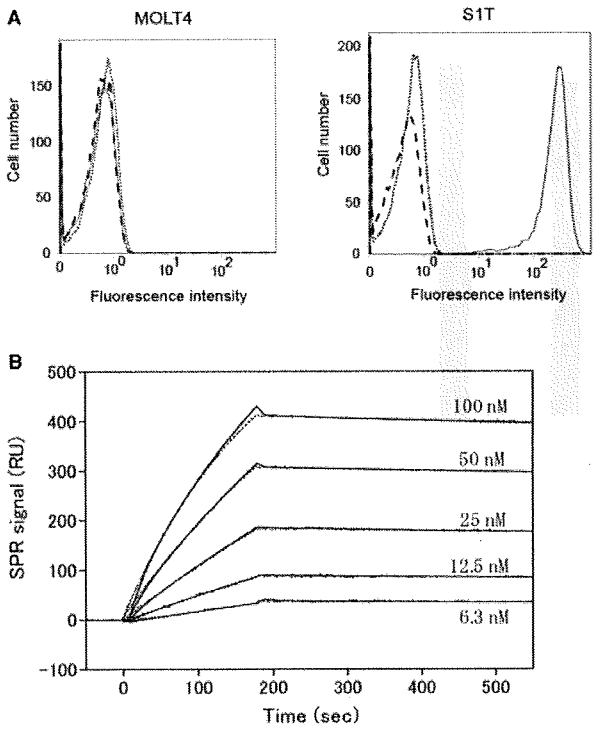

Fig. 9. **Binding analysis of S1T-A3 $(scFv)_2$-Fc to S1T cells on FACS (A) and to HLA-DR molecules by surface plasmon resonance (SPR) analysis (B).** The cells were stained with $(scFv)_2$-Fc, biotinylated anti-human Fc mAb and PE-labelled streptavidin (SA) (thick line). The dotted and broken lines indicate the data for staining without $(scFv)_2$-Fc and the cells only. The relative mean fluorescence (RMF) values of $(scFv)_2$-Fc to S1T and MOLT4 were 311 and 0.8, respectively. SPR analysis was performed on BIAcore 2000 (GE Healthcare) at 25°C and a flow rate of 20 µl/min. The HLA-DR molecules were conjugated to a CM5 sensorchip by the amine-coupling method. The $(scFv)_2$-Fc solution was injected to the flow cells at the indicated concentrations to monitor the association phase and the subsequent dissociation phase by eluting with the running buffer. The kinetic parameters of the binding were evaluated on BIAevaluation 3.2 software assuming a 1:1 binding model to give a dissociation equilibrium constant, K_d of 1.9 nM (k_a, association rate constant: $5.2 \times 10^4\ M^{-1}s^{-1}$, K_d, dissociation constant: $9.6 \times 10^{-5}\ s^{-1}$). The simulation curves calculated on the basis of these parameters were indicated in the dotted lines.

ATL cells (*13*, *23*). We demonstrated here that HLA-DR could be a candidate of clinical target for antibody therapy to ATL and that anti-HLA-DR antibody can work effectively to induce the cell death to ATL cell lines in addition to B-cell lymphoma, although its cell killing activity is largely dependent on the expression level of HLA-DR on the cells (Fig. 10).

1D10 (Hu1D10), a human IgG4 antibody isolated from the synthetic human antibody phage library (HuCal) induces apoptosis by a caspase-independent pathway without the aid of effector cells (*21*). However, as described by van der Neut Kolfschoten *et al.* (*24*) as IgG4 antibodies exchange Fab arms by swapping a heavy chain and attached light chain with a heavy-light chain pair from another molecule, such swapping mechanism might reduce efficacy of 1D10. Anti-HLA-DR human antibody HD8 generated by transchromo mouse technology also exhibited cell cytotoxic activity through the effecter cells or the complement (*22*). Other antibodies were used for killing malignant lymphocytes by exerting anti-tumour activity through cell-death signalling (*21*, *22*, *25–27*).

As compared with these whole antibodies, small fragment antibodies like scFv or minibodies are considered to have several advantages in clinical applications. These include easy control of serum concentration owing to their short half-life in serum, high penetration into target tissues owing to their small sizes, low cost of production using bacterial cells and less side-effects such as antibody (Fc)- or complement-dependent cytotoxicity against the normal cells. Kimura *et al.* (*28*) described a diabody with agonistic activity to induce apoptosis through the ligation of MHC class I molecules by a caspase-independent pathway. This diabody (2D7) showed a 4-fold stronger apoptotic activity on ARH-77 cells (a myeloma cell line) than the original whole antibody 2D7 dimerized by anti-mouse Fc Ab. In our case, the S1T-A3 diabody specific to MHC class II molecules also had 15-fold higher cell-death activity than the $(scFv)_2$-Fc or L243 mouse whole antibody (Fig. 8). These results suggest that the death signalling through MHC class I or II molecules is more effectively exerted by the diabody form rather than by the whole antibody or the $(scFv)_2$-Fc form.

The features of the cell death induced by the S1T-A3 diabody were characterized by PI- and Annexin V- double positive staining on FACS analysis (Fig. 5), which indicates not a typical apoptosis but apoptosis-like cell death with necrotic feature. The similar properties of the cell death by HLA-DR signalling were reported in B-cell lymphoma characterized by caspase-independent pathway (*21*) with accompanying DNA fragmentation (*29*). Recently, Carlo-Stella *et al.* (*30*) proposed another cell-death pathway. The humanized anti-HLA-DR antibody 1D09C3 exerts a potent anti-tumour effect on the chronic lymphocytic leukaemia JVM-2 and the mantle-cell lymphoma cell line GRANTA-519 by activating reactive oxygen species-dependent, c-Jun-NH2-kinase (JNK)-driven cell death. The other paper described that the HLA-DR/CD18 complex stimulated by L243 mAb ligation delivers the cell death signalling through the activation of protein kinase C (PKC) β which is located in the outside of the lipid raft of the cell surface (*31*). Thus, several papers as for signalling pathway of cell death through HLA-DR reported somewhat contradictory results. S1T-A3 diabody exerting an effective anti-tumour activity by a strong cell death may contribute to understanding the cell-death-signalling pathway through HLA-DR.

Based on the earlier findings that CCR4 expression is associated with ATLL (Adult T-cell leukaemia/lymphoma) at a high frequency (88%) (*32*), an anti-CCR4 Ab is under development for ATL treatment (*33*). When using therapeutic agents, which target a single pathogenic marker of the tumour, the appearance of relapses or refractory tumours is problematic. In fact, despite the clinical success of rituximab (anti CD20 mAb), relapse of CD20-negative tumours have been

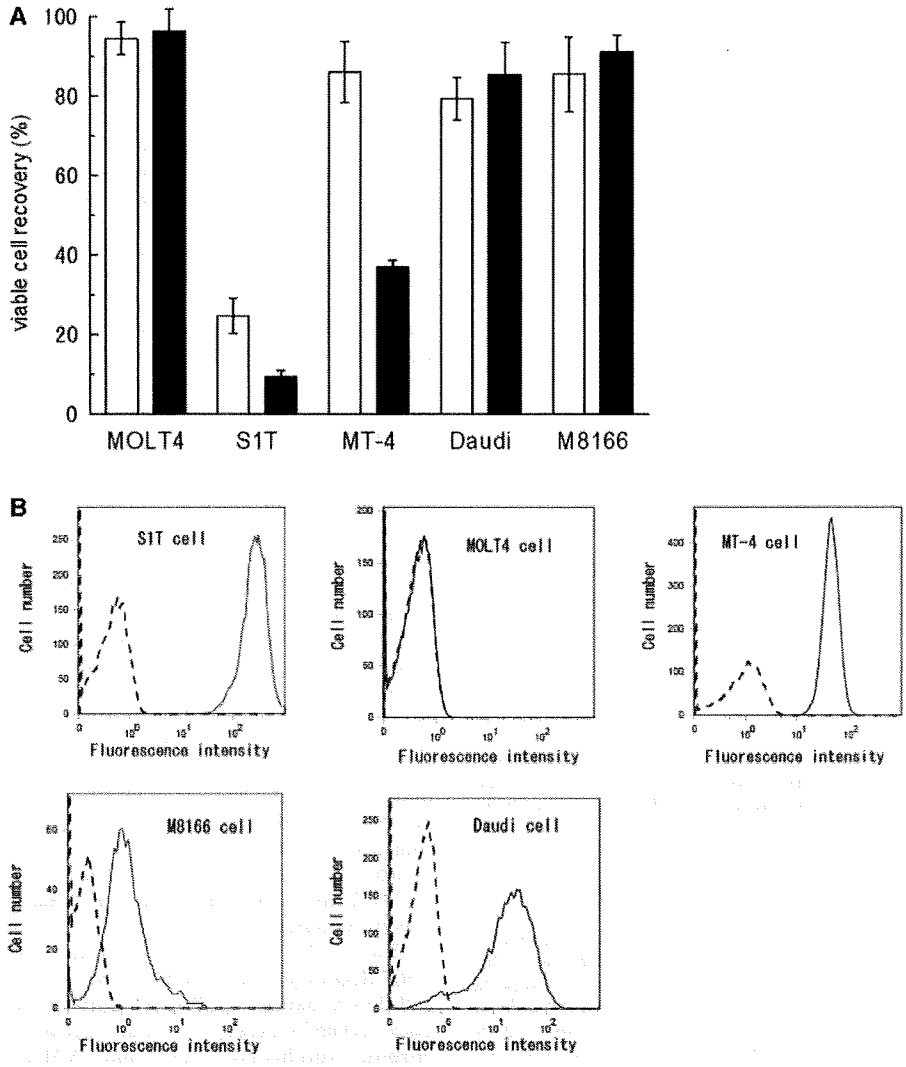

Fig. 10. **Cell-death-inducing activities of S1T-A3 diabody on S1T, MOLT4, Daudi and M8166 and MT-4 cell lines (A) and the expression levels of HLA-II molecules on each cell (B).** The open and filled bars in (A) indicate the viable cell recovery (%) of each cell lines treated with anti HLA-DR α chain mAb L243 (200 nM) and S1T-A3 diabody (60 nM), respectively. S1T-A3 diabody used here are the scFv dimer with GGGGS linker. The expression of HLA molecules in (B) was analysed by staining with L243mAb on FACS. The relative mean fluorescence (RMF) of S1T, MT-4, MOLT4, M8166 and Daudi cells were estimated to be 520, 72, 1.0, 4.0 and 55 respectively.

reported (*34*). Recently, we reported that CD70 is a promising tumour marker for ATL (*13*). We are expecting the anti-HLA-DR diabody to provide an alternative candidate for antibody therapy for ATL with a distinct targets and mechanism of action, together with the anti-CCR4 and anti-CD70 antibodies.

FUNDING

A grant from the Frontier Science Research Center, Kagoshima University; a grant from Japan Science and Technology Agency; and a Grant-in-Aid for Scientific Research (B) from the Japan Society for the Promotion of Science (grant no. 19390153).

CONFLICT OF INTEREST

None declared.

REFERENCES

1. Matsuoka, M. and Jeang, K.T. (2005) Human T-cell leukemia virus type I at age 25: a progress report. *Cancer Res.* **65**, 4467–4470
2. Ohshima, K. (2007) Pathological features of diseases associated with human T-cell leukemia virus type I. *Cancer Sci.* **98**, 772–778
3. Hoogenboom, H.R. (2005) Selecting and screening recombinant antibody libraries. *Nat. Biotechnol.* **23**, 1105–1116
4. Jakobovits, A., Amado, R.G., Yang, X., Roskos, L., and Schwab, G. (2007) From XenoMouse technology to

panitumumab, the first fully human antibody product from transgenic mice. *Nat. Biotechnol.* **25**, 1134–1143
5. Ridgway, J.B., Ng, E., Kern, J.A., Lee, J., Brush, J., Goddard, A., and Carter, P. (1999) Identification of a human anti-CD55 single-chain Fv by subtractive panning of a phage library using tumor and nontumor cell lines. *Cancer Res.* **59**, 2718–2723
6. McWhirter, J.R., Kretz-Rommel, A., Saven, A., Maruyama, T., Potter, K.N., Mockridge, C.I., Ravey, E.P., Qin, F., and Bowdish, K.S. (2006) Antibodies selected from combinatorial libraries block a tumor antigen that plays a key role in immunomodulation. *Proc. Natl Acad. Sci. USA.* **103**, 1041–1046
7. Giordano, R.J., Cardo-Vila, M., Lahdenranta, J., Pasqualini, R., and Arap, W. (2001) Biopanning and rapid analysis of selective interactive ligands. *Nat. Med.* **7**, 1249–1253
8. de Kruif, J., Terstappen, L., Boel, E., and Logtenberg, T. (1995) Rapid selection of cell subpopulation-specific human monoclonal antibodies from a synthetic phage antibody library. *Proc. Natl Acad. Sci. USA* **92**, 3938–3942
9. Watters, J.M., Telleman, P., and Junghans, R. P. (1997) An optimized method for cell-based phage display panning. *Immunotechnology* **3**, 21–29
10. Mutuberria, R., Satijn, S., Huijbers, A., Van Der Linden, E., Lichtenbeld, H., Chames, P., Arends, J.W., and Hoogenboom, H.R. (2004) Isolation of human antibodies to tumor-associated endothelial cell markers by in vitro human endothelial cell selection with phage display libraries. *J. Immunol. Methods* **287**, 31–47
11. Roovers, R.C., van der Linden, E., de Bruine, A.P., Arends, J.W., and Hoogenboom, H.R. (2001) Identification of colon tumour-associated antigens by phage antibody selections on primary colorectal carcinoma. *Eur. J. Cancer* **37**, 542–549
12. Sakaki, Y., Terashi, K., Yamaguchi, A., Kawamata, N., Tokito, Y., Mori, H., Umehara, M., Yoshiyama, T., Ohtsubo, H., Arimura, K., Arima, N., and Tei, C. (2002) Human T-cell lymphotropic virus type I Tax activates lung resistance-related protein expression in leukemic clones established from an adult T-cell leukemia patient. *Exp. Hematol.* **30**, 340–345
13. Baba, M., Okamoto, M., Hamasaki, T., Horai, S., Wang, X., Ito, Y., Suda, Y., and Arima, N. (2008) Highly enhanced expression of CD70 on human T-lymphotropic virus type 1-carrying T-cell lines and adult T-cell leukemia cells. *J. Virol.* **82**, 3843–3852
14. Hashiguchi, S., Nakashima, T., Nitani, A., Yoshihara, T., Yoshinaga, K., Ito, Y., Maeda, Y., and Sugimura, K. (2003) Human Fc epsilon RIalpha-specific human single-chain Fv (scFv) antibody with antagonistic activity toward IgE/Fc epsilon RIalpha-binding. *J. Biochem.* **133**, 43–49
15. Hamasaki, T., Hashiguchi, S., Ito, Y., Kato, Z., Nakanishi, K., Nakashima, T., and Sugimura, K. (2005) Human anti-human IL-18 antibody recognizing the IL-18-binding site 3 with IL-18 signaling blocking activity. *J. Biochem.* **138**, 433–442
16. Maeda, H., Matsushita, S., Eda, Y., Kimachi, K., Tokiyoshi, S., and Bendig, M.M. (1991) Construction of reshaped human antibodies with HIV-neutralizing activity. *Hum. Anitibodies Hybridomas* **2**, 124–134
17. Arakawa, T., Philo, J.S., Ejima, D., Tsumoto, K., and Arisaka, F. (2006) Aggregation Analysis of Therapeutic Proteins, Part 1. *Gen. Asp. Tech. Assess. BioProcess Int.* **4**, 32–43
18. Higuchi, M., Matsuda, T., Mori, N., Yamada, Y., Horie, R., Watanabe, T., Takahashi, M., Oie, M., and Fujii, M. (2005) Elevated expression of CD30 in adult T-cell leukemia cell lines: possible role in constitutive NF-kappaB activation. *Retrovirology* **2**, 29
19. Lang, P., Stolpa, J.C., Freiberg, B.A., Crawford, F., Kappler, J., Kupfer, A., and Cambier, J.C. (2001) TCR-induced transmembrane signaling by peptide/MHC class II via associated Ig-alpha/beta dimers. *Science* **291**, 1537–1540
20. Trautmann, A. and Valitutti, S. (2003) The diversity of immunological synapses. *Curr. Opin. Immunol.* **15**, 249–254
21. Nagy, Z.A., Hubner, B., Lohning, C., Rauchenberger, R., Reiffert, S., Thomassen-Wolf, E., Zahn, S., Leyer, S., Schier, E. M., Zahradnik, A., Brunner, C., Lobenwein, K., Rattel, B., Stanglmaier, M., Hallek, M., Wing, M., Anderson, S., Dunn, M., Kretzschmar, T., and Tesar, M. (2002) Fully human, HLA-DR-specific monoclonal antibodies efficiently induce programmed death of malignant lymphoid cells. *Nat. Med.* **8**, 801–807
22. Tawara, T., Hasegawa, K., Sugiura, Y., Tahara, T., Ishida, I., and Kataoka, S. (2007) Fully human antibody exhibits pan-human leukocyte antigen-DR recognition and high in vitro/vivo efficacy against human leukocyte antigen-DR-positive lymphomas. *Cancer Sci.* **98**, 921–928
23. Shirono, K., Hattori, T., Hata, H., Nishimura, H., and Takatsuki, K. (1989) Profiles of expression of activated cell antigens on peripheral blood and lymph node cells from different clinical stages of adult T-cell leukemia. *Blood* **73**, 1664–1671
24. van der Neut Kolfschoten, M., Schuurman, J., Losen, M., Bleeker, W.K., Martinez-Martinez, P., Vermeulen, E., den Bleker, T.H., Wiegman, L., Vink, T., Aarden, L.A., De Baets, M.H., van de Winkel, J.G., Aalberse, R.C., and Parren, P.W. (2007) Anti-inflammatory activity of human IgG4 antibodies by dynamic Fab arm exchange. *Science* **317**, 1554–1557
25. Bertho, N., Blancheteau, V.M., Setterblad, N., Laupeze, B., Lord, J.M., Drenou, B., Amiot, L., Charron, D.J., Fauchet, R., and Mooney, N. (2002) MHC class II-mediated apoptosis of mature dendritic cells proceeds by activation of the protein kinase C-delta isoenzyme. *Int. Immunol.* **14**, 935–942
26. Shan, D., Ledbetter, J.A., and Press, O.W. (2000) Signaling events involved in anti-CD20-induced apoptosis of malignant human B cells. *Cancer Immunol. Immunother.* **48**, 673–683
27. Ghetie, M.A., Podar, E.M., Ilgen, A., Gordon, B.E., Uhr, J.W., and Vitetta, E.S. (1997) Homodimerization of tumor-reactive monoclonal antibodies markedly increases their ability to induce growth arrest or apoptosis of tumor cells. *Proc. Natl Acad. Sci. USA* **94**, 7509–7514
28. Kimura, N., Kawai, S., Kinoshita, Y., Ishiguro, T., Azuma, Y., Ozaki, S., Abe, M., Sugimoto, M., Hirata, Y., Orita, T., Okabe, H., Matsumoto, T., and Tsuchiya, M. (2004) 2D7 diabody bound to the alpha2 domain of HLA class I efficiently induces caspase-independent cell death against malignant and activated lymphoid cells. *Biochem. Biophy.s Res. Commun.* **325**, 1201–1209
29. Drenou, B., Blancheteau, V., Burgess, D.H., Fauchet, R., Charron, D.J., and Mooney, N. A. (1999) A caspase-independent pathway of MHC class II antigen-mediated apoptosis of human B lymphocytes. *J. Immunol.* **163**, 4115–4124
30. Carlo-Stella, C., Di Nicola, M., Turco, M. C., Cleris, L., Lavazza, C., Longoni, P., Milanesi, M., Magni, M., Ammirante, M., Leone, A., Nagy, Z., Gioffre, W.R., Formelli, F., and Gianni, A.M. (2006) The anti-human leukocyte antigen-DR monoclonal antibody 1D09C3 activates the mitochondrial cell death pathway and exerts a potent antitumor activity in lymphoma-bearing nonobese diabetic/severe combined immunodeficient mice. *Cancer Res.* **66**, 1799–1808
31. Doisne, J.M., Castaigne, J.G., Deruyffelaere, C., Dieu-Nosjean, M.C., Chamot, C., Alcaide-Loridan, C., Charron, D., and Al-Daccak, R. (2008) The context of HLA-DR/CD18 complex in the plasma membrane governs

HLA-DR-derived signals in activated monocytes. *Mol. Immunol.* **45**, 709–718
32. Ishida, T., Inagaki, H., Utsunomiya, A., Takatsuka, Y., Komatsu, H., Iida, S., Takeuchi, G., Eimoto, T., Nakamura, S., and Ueda, R. (2004) CXC chemokine receptor 3 and CC chemokine receptor 4 expression in T-cell and NK-cell lymphomas with special reference to clinicopathological significance for peripheral T-cell lymphoma, unspecified. *Clin Cancer Res.* **10**, 5494–5500
33. Murata, K. and Yamada, Y. (2007) The state of the art in the pathogenesis of ATL and new potential targets associated with HTLV-1 and ATL. *Int. Rev. Immunol.* **26**, 249–268
34. Jazirehi, A.R. and Bonavida, B. (2005) Cellular and molecular signal transduction pathways modulated by rituximab (rituxan, anti-CD20 mAb) in non-Hodgkin's lymphoma: implications in chemosensitization and therapeutic intervention. *Oncogene* **24**, 2121–2143
35. Brochet, X., Lefranc, M P., and Giudicelli, V. (2008) IMGT/V-QUEST: the highly customized and integrated system for IG and TR standardized V-J and V-D-J sequence analysis. *Nucleic Acids Res.* **36**, W503–W508